Hindawi
Geofluids
Volume 2022, Article ID 5778761, 25 pages
https://doi.org/10.1155/2022/5778761

Research Article

Study on Stress-Strain Characteristics of Pipeline-Soil Interaction under Ground Collapse Condition

Xiaohui Liu,[1,2] **Zhizhong Sun**,[3] **Jianping Zhu**,[2] **Yingchao Fang**,[2] **Yanglian He**,[2] **and Yuchen Pan**[4]

[1]*School of Civil Engineering and Mechanics, Lanzhou University, Lanzhou, Gansu 730000, China*
[2]*National Petroleum and Natural Gas Pipeline Group Southwest Pipeline Company, Chengdu, Sichuan 610000, China*
[3]*Institute of Geological Natural Disaster Prevention and Control, Gansu Academy of Sciences, Lanzhou, Gansu 730000, China*
[4]*State Key Laboratory of Geohazard Prevention and Geoenvironment Protection, Chengdu University of Technology, Chengdu, Sichuan 610000, China*

Correspondence should be addressed to Zhizhong Sun; szz-1983@163.com

Received 18 April 2022; Revised 9 June 2022; Accepted 7 July 2022; Published 4 August 2022

Academic Editor: Meng Jingjing

Ground collapse is one of the main geological disasters affecting the safe operation of oil and gas pipelines. Studying the stress-strain characteristics of pipe-soil interaction under ground collapse has an important guiding role for the prevention of ground collapse and the safety protection of pipelines. The current results are mostly concentrated in a single theory or the stress of the pipeline itself, which cannot fully consider the pipe-soil interaction. In this paper, ABAQUS is used to establish the finite element geometric model. Considering the pipeline and the surrounding geological environment conditions, the study is carried out from five aspects: the length of the collapse area, the thickness of the cover layer, the buried depth of the pipeline, the diameter of the pipeline, and the thickness of the pipeline. The displacement of the pipeline soil, the deformation of the pipeline, and the characteristics of the pipeline stress are analyzed, and the variation law is determined through the development trend of the pipeline stress and strain. At the same time, by fitting and analyzing the relationship between the span of different subsidence areas, the thickness of the cover layer, the buried depth of the pipeline, the diameter of the pipeline, the thickness of the pipeline, and the maximum deformation of the pipeline, the reference value of the maximum subsidence displacement of the pipeline under the action of ground collapse is proposed. The work has practical application value for pipeline monitoring, early warning, and disaster management.

1. Introduction

Ground collapse refers to a geological phenomenon wherein surface rock-soil mass fall downward under the action of natural or human factors and form collapse pits (holes) on the ground [1]. In recent years, with the rapid development of oil and gas pipelines, more and more oil and gas pipelines cross the ground subsidence area, such as the China-Myanmar pipeline and West-East Gas Pipeline. Oil and gas pipelines are affected by the external load of ground subsidence, resulting in pipeline deformation, suspension, local deformation, or stress concentration, which leads to large displacement, buckling or creep, and even pipeline fracture cand failure, which poses a serious threat to the safe operation of pipelines [2–7]. For example, in July 2011, the Qingdao natural gas pipeline was continuously exposed due to ground subsidence, and it lost fulcrum and leaked. In January 2020, a large area of pavement collapsed suddenly in front of Xining bus station, and many power pipelines, communication pipelines, and natural gas pipelines were damaged [8–10]. In order to avoid the harm and influence of ground collapse on oil and gas pipelines and ensure the long-term safety of energy channels, scientific and effective methods should be adopted to accurately analyze the law of pipe-soil interaction under ground collapse conditions, which is the key basis for monitoring prevention and engineering treatment measures [11, 12].

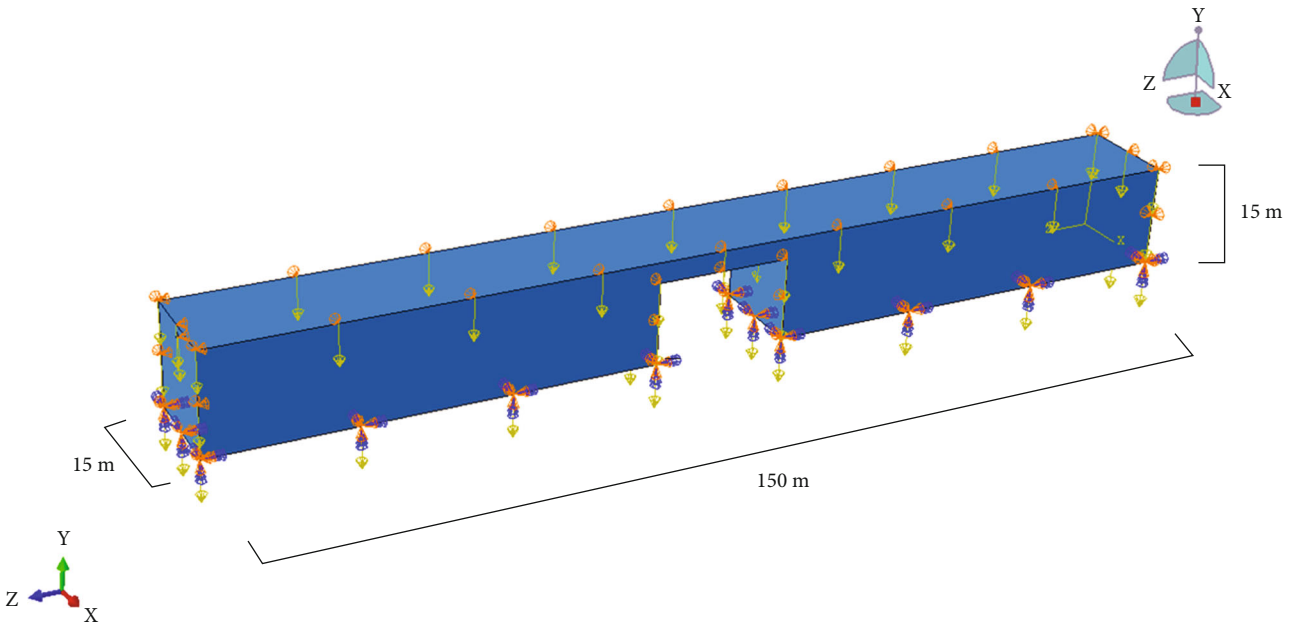

Figure 1: Finite element calculation model.

Table 1: Pipeline parameters.

Pipeline	Diameter (mm)	Wall thickness (mm)	Density (kg/m^3)	Elastic modulus (GPa)	Poisson ratio	Internal pressure (MPa)	Minimum yield strength (MPa)
X80	1016	18.4	7850	207	0.3	8~14	555~675

Table 2: Soil parameters.

Soil parameters	Elastic modulus (MPa)	Poisson	Density (kg/m^3)	Angle of internal friction (°)	Expansion angle (°)	Flow stress ratio
Soil mass	32.5	0.3	2040	25	0	1

Domestic and foreign scholars have conducted modeling and theoretical research on the stress of buried pipelines. Muleski et al. [13] established the shell model of buried pipeline under seismic environment and analyzed the buckling and fracture stress of buried pipeline by using the coupled equilibrium equation. Yun and Kyriakides [14] established the torsional beam model of buried pipeline and analyzed the ultimate load of buried pipeline by considering the actual parameters of the pipeline. Shmulevich and Galili [15] carried out an experimental comparison of pipelines with different degrees of stiffness by designing soil boxes, focusing on the analysis of normal stress and tangential stress of pipelines. Based on the Winkler model and elastic continuous medium, Klar et al. studied the differences of interaction between pipeline and soil under the condition of tunnel excavation [16]. Adeeb and Horsley established a numerical calculation method for the safety working pressure of rock ditch pipeline excavation and determined the safety working pressure of pipeline excavation [17]. Kinash and Najafi simplified the response of the thin-walled cylinder pipe under combined load and internal pressure into a one-dimensional model by using the plastic theory and thin film theory of shell and discussed the influence of internal pressure, bending moment, and longitudinal force on the stress-strain distribution of the straight pipe [18]. Saiyar et al. proposed a joint simplified design formula for bending moment transfer and bending moment release of the flexible pipe and analyzed the factors that control the structural response of flexible pipe joints [19]. Shruthi studied the seismic response of buried pipelines and the design of seismic connection structure and used software to simulate the response of corresponding areas [20]. Varianou et al. established a risk assessment system for oil and gas pipelines based on the quantitative risk analysis method and made a comprehensive risk assessment of the stress and deformation of oil and gas pipelines [21]. Wu et al. studied the mechanical properties of DN110 polyethylene buried pipe with scratch defects under the condition of land subsidence and established the functional relationship model between land subsidence displacement and other parameters [22]. Wang et al. proposed the time-dependent limit state equation of suspended pipeline considering corrosion defects and established the nonprobabilistic time-dependent reliability model, which greatly promoted the assessment standard of suspended pipeline with corrosion

Table 3: Simulated conditions.

Influencing factor	Factors of collapse area		Pipeline factors		
	Collapse length (m)	Cover layer thickness (m)	Buried depth (m)	Pipeline diameter (mm)	Wall thickness (mm)
Collapse length	20	4	1	1016	18.4
	40	4	1	1016	18.4
	80	4	1	1016	18.4
	120	4	1	1016	18.4
Cover layer thickness	40	4	1	1016	18.4
	40	6	1	1016	18.4
	40	8	1	1016	18.4
	40	10	1	1016	18.4
Buried depth	40	4	0.5	1016	18.4
	40	4	1	1016	18.4
	40	4	1.5	1016	18.4
	40	4	2	1016	18.4
Pipeline diameter	40	4	1	610	18.4
	40	4	1	914	18.4
	40	4	1	1016	18.4
	40	4	1	1219	18.4
Wall thickness	40	4	1	1016	7.9
	40	4	1	1016	16.2
	40	4	1	1016	18.4
	40	4	1	1016	20.6

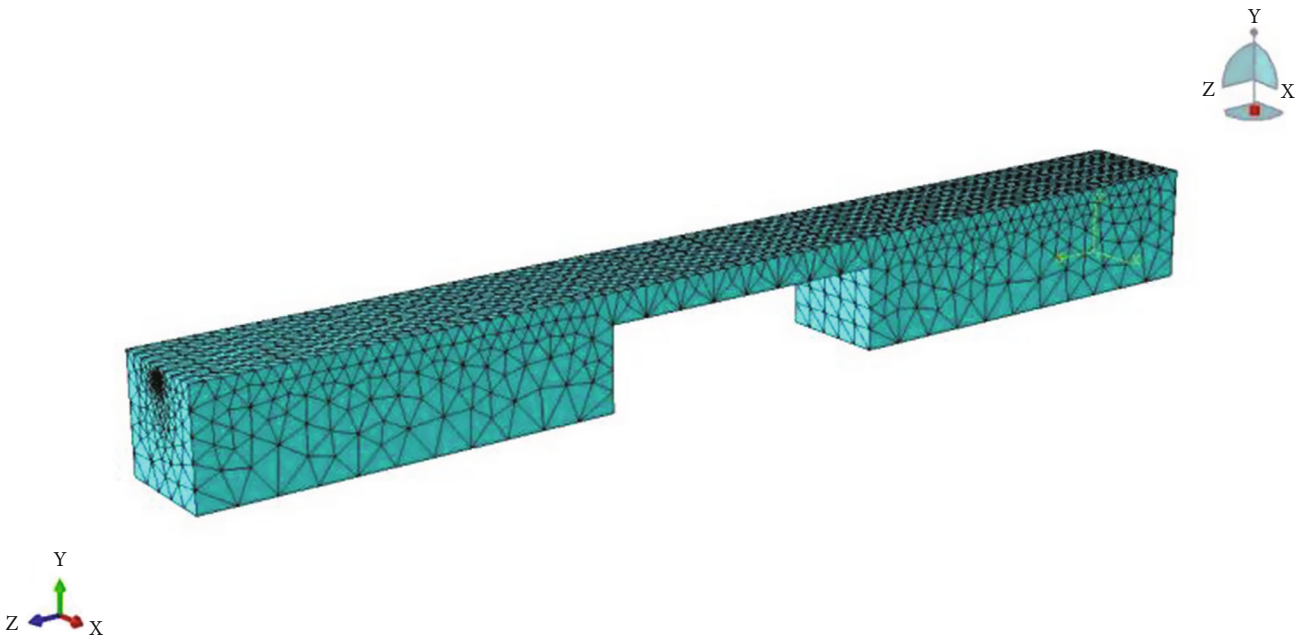

Figure 2: Grid division.

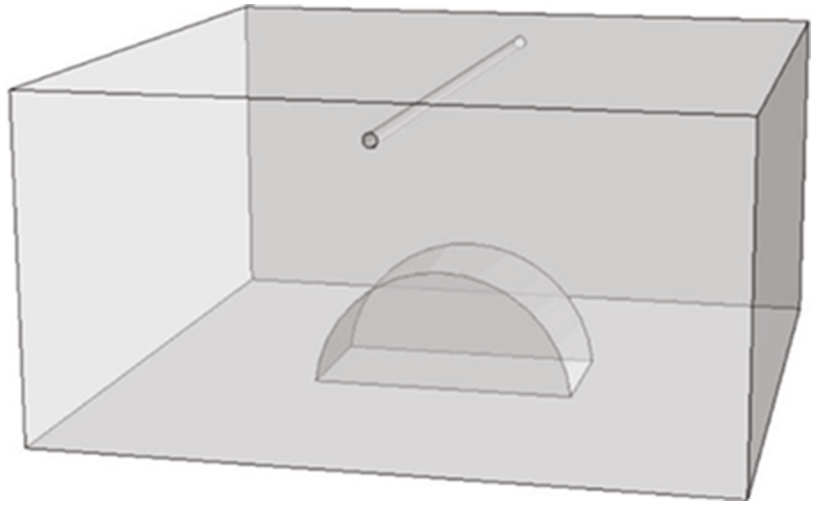

Figure 3: Model diagram.

Table 4: Relative error of maximum von Mises equivalent stress.

Cave collapse radius (m)	Maximum von Mises equivalent stress (MPa)		Relative error
	Original numerical solution	Numerical solution of literature	
10	17.28	18.5	6.61%
15	55.67	58.4	4.67%
20	101.728	110.0	7.52%

defects [23]. Wong et al. proposed a methodology to estimate pipeline strain under axial load caused by the moving slopes and applied this method to a case study to verify its reliability [24]. However, the current research results mainly focus on the establishment of models of stress strain of pipelines and rarely combine the safe operation of oil and gas pipelines, especially the research results on the stress-strain of pipelines with ground collapse [25–29].

In this paper, ABAQUS finite element software is used. Combined with pipeline operating conditions, geotechnical model, pipe model, and pipe-soil contact model, the stress model of pipeline under ground subsidence is established. The relationship between the span of the subsidence area, the thickness of the cover layer, the thickness of the pipeline wall, the buried depth, and the maximum deformation position and stress distribution of the pipeline is analyzed. The maximum displacement of the pipeline under different conditions is obtained, and the expression is fitted to determine the deformation and stress law of the pipeline, which can combine theory and practice to guide the safety management of oil and gas pipelines.

2. Numerical Study

2.1. Model Establishment. In this paper, the finite element geometric model is established by ABAQUS software. The size of the soil model in X, Y, Z directions is 15 m × 15 m × 150 m, and the distance between the pipeline center and surface is set according to different working conditions. In order to simplify the model, the collapse section is rectangular, and the whole collapse area is hollowed out, as shown in Figure 1.

This finite element model is established to study the deformation and failure mechanism of pipelines under the condition of ground collapse, and the influence of other secondary factors should be ignored. Therefore, the model assumes the following:

(1) It is assumed that the pipeline is not affected by other geological disasters in the process of pipe-soil interaction, and only the pipeline oil and gas transportation under the action of ground subsidence is considered

(2) It is assumed that the pipeline and soil are homogeneous and their mechanical properties are stable. The physical and mechanical properties are uniformly distributed along the axial direction of the pipeline

(3) The influence of temperature change, stress of initial material assembly, external vibration, and other objective factors are not considered

In this paper, a bilinear follow-up elastoplastic model is adopted. The pipeline material is X80 steel pipeline. σ_1 is 544 MPa, and E_2 is 6210 MPa. The relevant parameters are shown in Table 1. Soil parameters are shown in Table 2.

The strain law of soil is elastic deformation and plastic deformation. In this paper, the Mohr-Coulomb elastoplastic constitutive model is used to describe the mechanical properties of soil in finite element numerical simulation. The soil mechanics changes are accurately described mainly by three parameters: the internal friction angle, cohesion, and expansion friction angle of the soil. The shear stress on the force

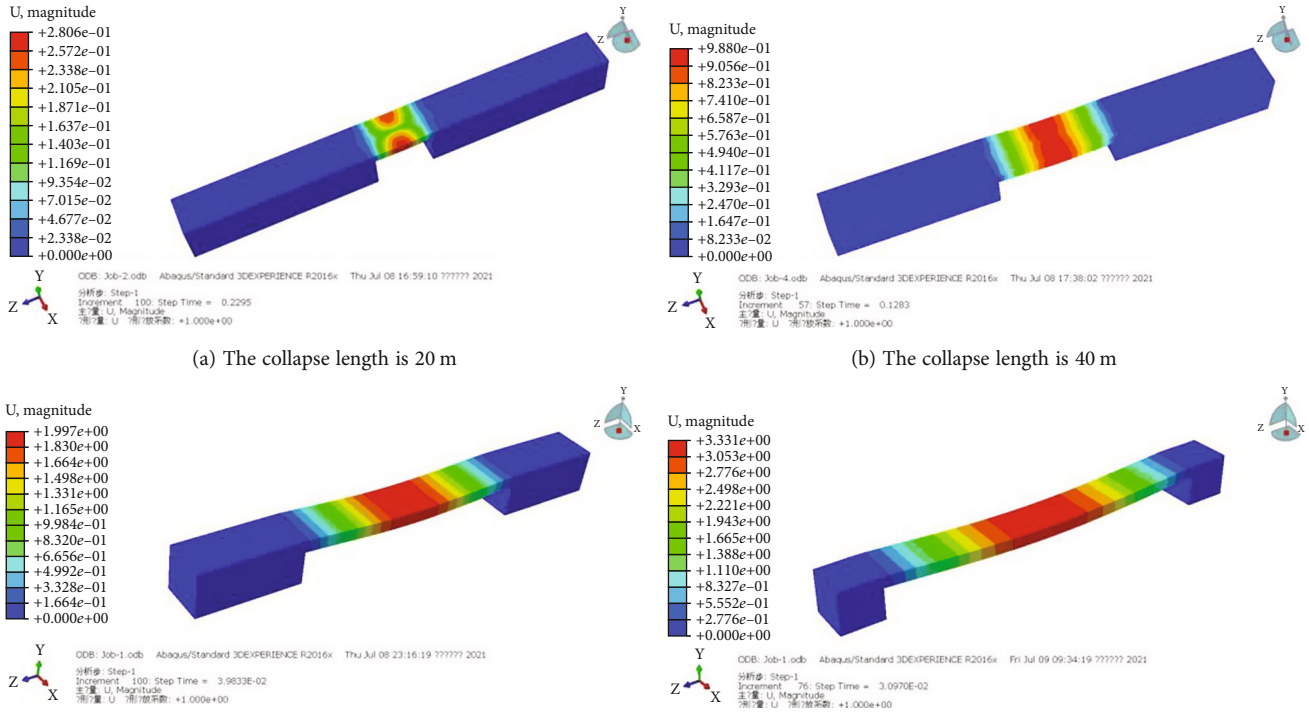

(a) The collapse length is 20 m

(b) The collapse length is 40 m

(c) The collapse length is 80 m

(d) The collapse length is 120 m

Figure 4: Soil displacement under different collapse lengths.

surface of the soil element is

$$\tau_n = c + \sigma_n \tan \varphi. \tag{1}$$

In the formula, σ_n and τ_n are the normal stress and shear stress on the rupture surface, respectively; c is the cohesion; and φ is the internal friction angle.

2.2. Boundary Conditions and Working Conditions. When the soil and pipeline interact, the interaction between the pipe and the soil is simulated by setting the contact surface between the pipe and the soil. The contact mode between the pipeline and soil is defined as the surface and surface contact. The advantages of this contact are manifested in supporting low-order and high-order elements of the surface, supporting large deformation of friction and sliding, and providing better contact effect. The outer surface of the pipe with higher stiffness is selected as the main surface, and the surface of the soil with lower stiffness is selected as the slave surface. The tangential behavior needs to consider the friction between the pipe and the soil. The friction formula is set as a penalty function, and the friction coefficient is 0.5. Hard contact is adopted in normal contact behavior, and the constraint execution method is in the default form.

The model considers the gravity effect. The upper surface of the soil is the free plane, and the bottom of the soil is completely fixed. Displacement and rotation angle are fixedly constrained around and are constrained to a certain value range. Both sides of the pipeline also use fixed constraint displacement and rotation angle, which are constrained to a certain value range and constrain the displacement change in the z direction.

In this paper, five factors including the collapse length, the thickness of the cover layer, the buried depth of the pipeline, the diameter of the pipeline, and the thickness of the pipeline are studied, and the simulation conditions are shown in Table 3.

2.3. Analysis Step and Meshing. The analysis algorithm is static, and the analysis step is set to 1. The numerical simulation of the pipeline and soil analyzed by ABAQUS belongs to nonlinear analysis. In order to make the numerical simulation easy to converge, the maximum increment step is set as 100. The initial increment is set to 0.001 and the maximum increment step is set to 0.08. The Field Output Manager for variables is strain, stress, and displacement. The History Export Manager selects the displacement variable used to export the displacement curve of the structure.

This paper adopts the method of splitting geometric elements in the software to split the model. For mesh division, the soil is divided freely, and the pipeline is divided by sweeping. In terms of shape, the pipeline is divided into quadrilateral meshes, and the soil layer is divided into regular tetrahedral meshes. Since the key parts of the calculation are the upper part of the model and the inside of the pipeline, the upper part and the pipeline mesh are finely divided. The division result is shown in Figure 2.

2.4. Model Verification. In view of the collapse geological disasters in buried pipeline engineering, Pan [30] took the pipe soil in karst collapse as the research object, analyzed the maximum von Mises equivalent stress of buried pipeline under different collapse radii of karst cave, and calculated the relative errors of the two modeling methods. The length

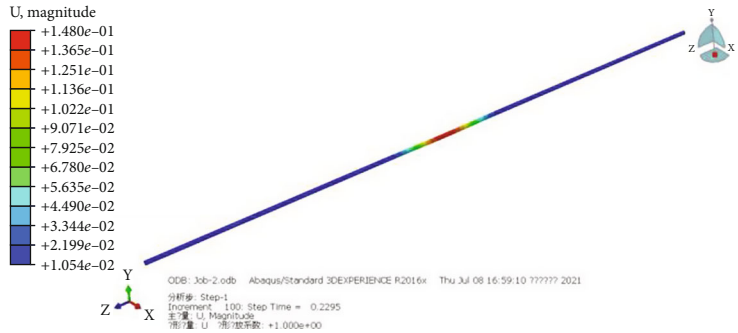

(a) The collapse length is 20 m

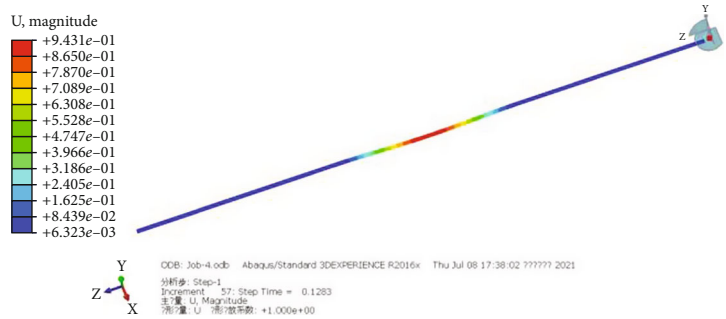

(b) The collapse length is 40 m

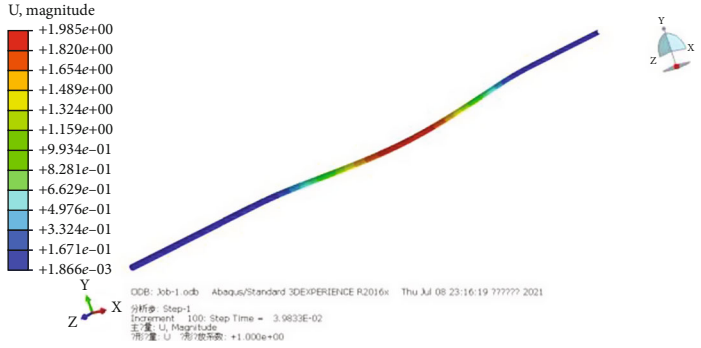

(c) The collapse length is 80 m

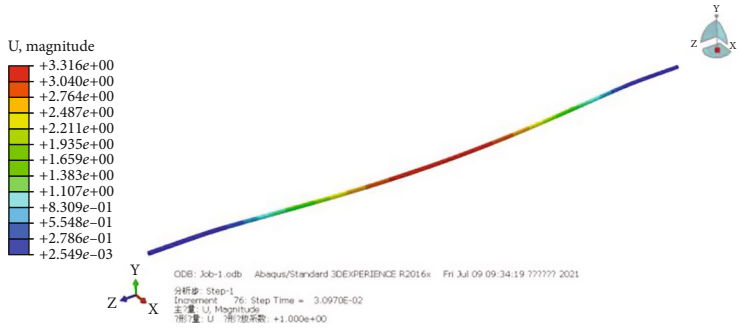

(d) The collapse length is 120 m

Figure 5: The pipeline ultimate deformation under different collapse lengths.

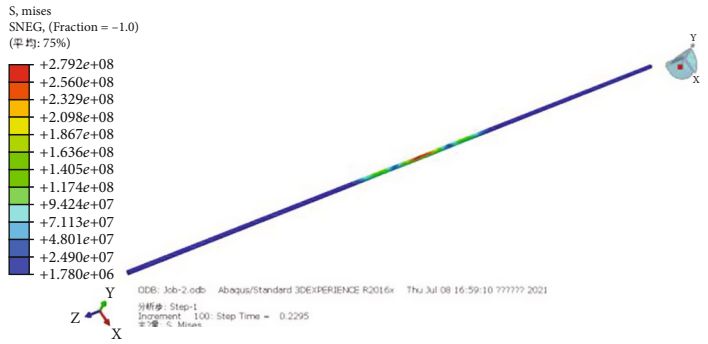

(a) The collapse length is 20 m

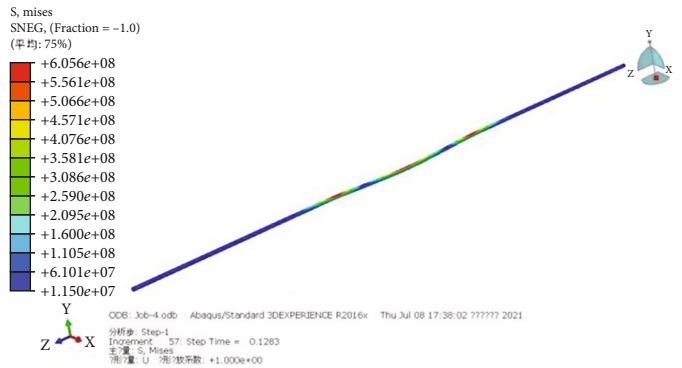

(b) The collapse length is 40 m

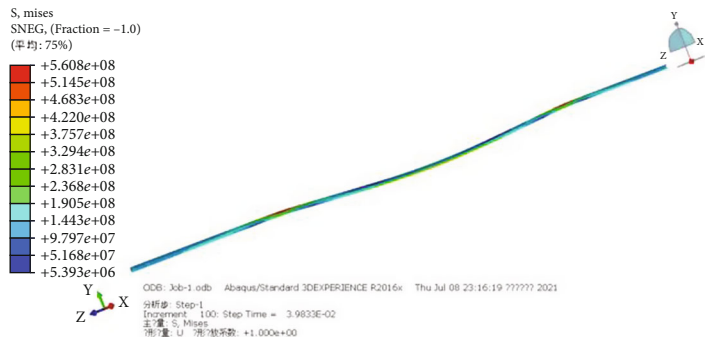

(c) The collapse length is 80 m

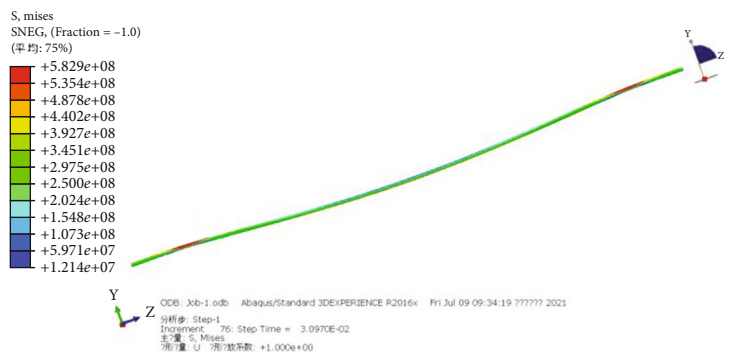

(d) The collapse length is 120 m

Figure 6: Pipeline stress under different collapse lengths.

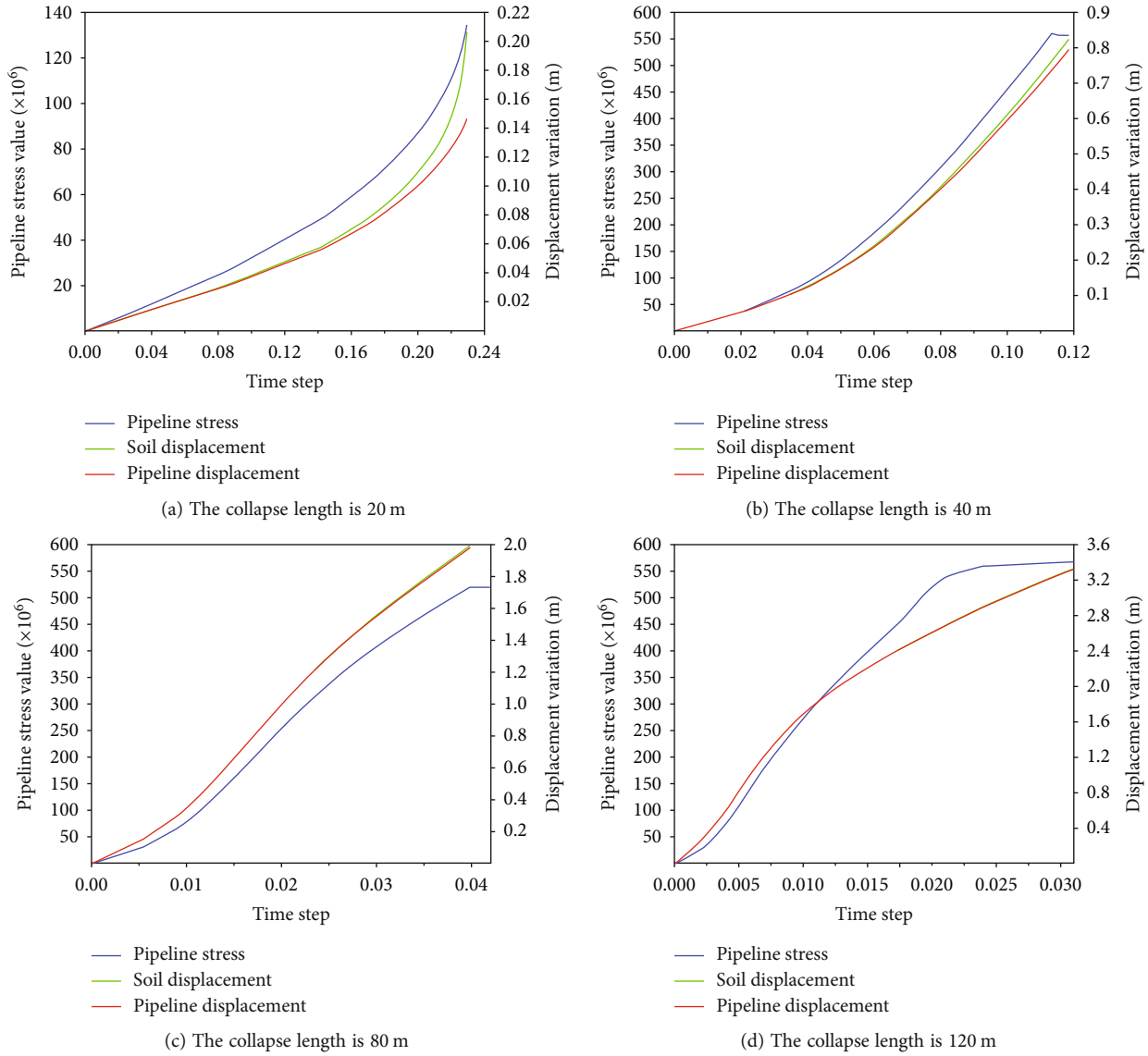

Figure 7: The diagrams of pipeline stress, displacement, and soil displacement under different collapse lengths.

of the karst cave model in the literature is 40 m, the thickness of the covering layer above the cave is 24 m, the buried depth of the pipeline is 1.5 m, the diameter of the pipe is 1016 mm, the thickness of the pipe is 17.5 mm, and the internal pressure of the pipe is 0.1 MPa. The model diagram is shown in Figure 3.

The numerical model of karst collapse is established according to the parameters in the above literature, and the comparison results are shown in Table 4. It can be seen that the error between the calculation results of the numerical model established by this method and those in the literature is small, and the rationality of the finite element model established is verified within an acceptable range.

3. Analysis of Deformation Stress Characteristics of Pipeline-Soil Interaction

3.1. Analysis on the Influence of Collapse Length. In order to study the influence of the ground collapse length on the pipeline stress, displacement, and soil displacement, finite element models with the collapse area lengths of 20 m, 40 m, 80 m, and 120 m were established for analysis.

3.1.1. Analysis of Soil Displacement under Different Collapse Lengths. Figure 4 is the nephograms of soil displacement under four different collapse lengths. When the length of the subsidence area is 20 m, the displacement of the soil on both sides of the pipeline in the subsidence area is large, and the displacement of the soil in the middle is small. This indicates that the pipeline exerts upward support on the soil. With the continuous increase of the collapse length, the center displacement of the subsidence area is increasing, and the force of the pipeline on the upper soil gradually loses its effect. When the collapse length is 20 m, the maximum displacement of the soil is 0.28 m. When the span reaches 120 m, the pipeline is damaged, and the maximum displacement reaches 3.31 m. With the continuous increase of the collapse length, the displacement of the soil in the collapse

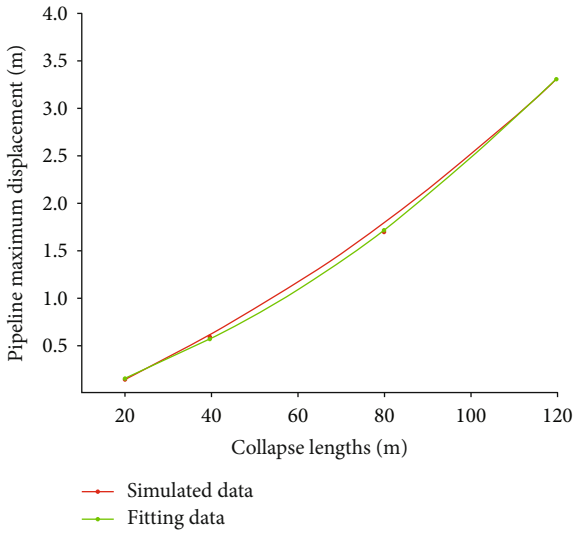

Figure 8: The pipeline maximum displacement under different collapse lengths.

area increases. The soil displacement first begins to deform from both sides of the center of the collapse area and finally forms a huge displacement change zone and then expands to both sides, resulting in collapse.

3.1.2. Analysis of Pipeline Ultimate Deformation under Different Collapse Lengths. Figure 5 shows the displacement nephograms of the pipeline under four different collapse lengths. The displacement nephograms of the pipeline are large in the middle and small in the two ends. With the increase of the span of the subsidence area, the pipeline deformation increases gradually. Like the soil displacement, it expands from the center of the pipe to both sides.

3.1.3. Analysis of Pipeline Stress under Different Collapse Lengths. Figure 6 shows the pipeline strain nephograms under different collapse lengths. Since the calculation is set to stop reaching the yield strength, the strain of the pipeline reaches the yield strength except that the collapse length is 20 m. When the collapse length is 20 m, the pipeline cannot reach the yield strength, and the pipeline is safe. It can be seen from the figures that the maximum strain of the pipeline is located in the contact point between the pipeline and the boundary of the collapse area and the middle of the pipeline. As the span increases, the pipeline strain increases as a whole. When the span is 120 m, the strain of the whole pipeline changes and even develops to both ends of the pipeline. If the length of the collapsed area of the pipeline is too large, the pipeline will not only be affected in the middle but also have changes at both ends.

The maximum displacement curves of soil and pipeline under different collapse lengths can be obtained by simulation calculation. The time step diagrams of pipeline stress, displacement, and soil displacement can be drawn (Figure 7), as well as the maximum displacement corresponding to different collapse lengths (Figure 8).

As shown in Figure 7, when the span of the subsidence area is 20 m, the strain and displacement have been increasing, the strain curve is close to vertical, and the calculation time step is far more than the time required for other working conditions, which leads to the automatic termination of the software calculation. It shows that when the span of the subsidence area is 20 m, the pipeline cannot reach the yield strength and will not be destroyed. Combined with the analysis of displacement nephograms, it is found that the ground subsidence soil under this span will be destroyed. There will be displacement changes in the pipeline, causing the possibility of exposed pipes. The growth rate of other displacement curves is slow at first and then rapid until the pipeline reaches the yield strength failure. The trend of stress and displacement curves is similar, and finally, the stress value tends to be stable, reaching the yield strength value. In the pipeline with the same buried depth, when the collapse length is very short, the deflection at both ends of the collapse area is small, and the pipeline cannot reach its maximum stress and strain. With the increase of the collapse length, the pipeline deflection increases, and the stress and strain increase. When the pipeline is long enough, the larger the overall stiffness is, the smaller the stress and strain the pipeline can reach.

According to the relationship diagram of the pipeline maximum displacement under different collapse lengths, formula (2) is obtained by data fitting, and the fitting degree is 0.997, indicating that the fitting effect is better. It can be seen that both are in a linear growth relationship. It can be seen from the curve that with the increase of the collapse length, the maximum displacement of the pipeline gradually increases, and its increasing speed eventually tends to be stable, which has a certain linear relationship.

$$f(x) = 0.000138x^2 + 0.01214x - 0.1386. \quad (2)$$

3.2. Analysis on the Influence of the Cover Layer Thickness. In order to study the influence of different thicknesses of soil cover layer on pipeline stress, displacement, and soil displacement under the action of ground subsidence, four finite element models of 4 m, 6 m, 8 m, and 10 m thickness of soil cover layer are established, and the parameters remain unchanged.

3.2.1. Analysis of Soil Displacement under Different Cover Layer Thicknesses. Figure 9 shows the soil displacement nephograms of four different cover layer thicknesses. It can be seen that the change of soil displacement is positively correlated with the thickness of the cover layer. With the increase of thickness, the deformation of the collapse area expands from the center to both sides, begins to deform from both sides of the lower edge of the cover layer, slowly develops to the whole soil cover layer, and finally forms collapse. With the increase of the cover layer thickness, when the pipeline reaches yield strength, the maximum displacement of soil can reach 1.15 m, and the minimum displacement is 0.82 m.

3.2.2. Analysis of Pipeline Ultimate Deformation under Different Cover Layer Thicknesses. Figure 10 shows the displacement nephograms of pipelines under four different cover layer thicknesses. The numerical variation of pipeline

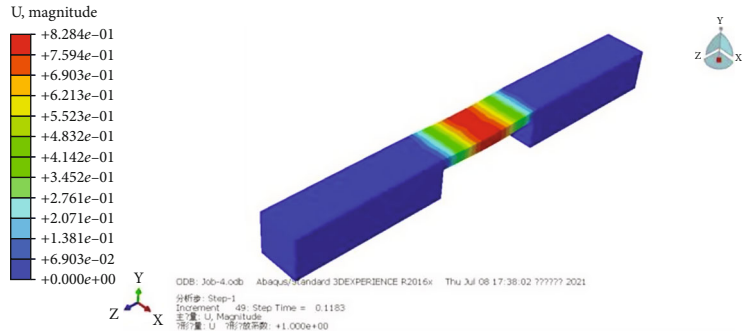

(a) The soil cover layer thickness is 4 m

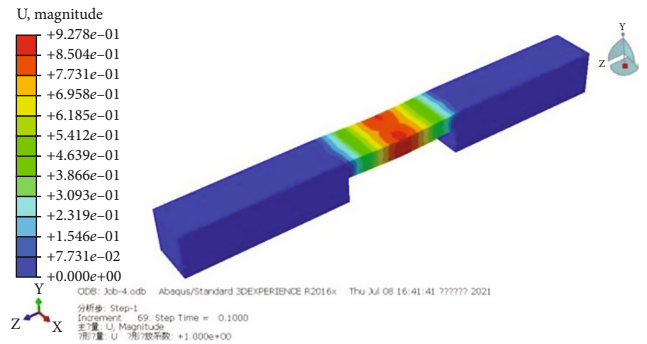

(b) The soil cover layer thickness is 6 m

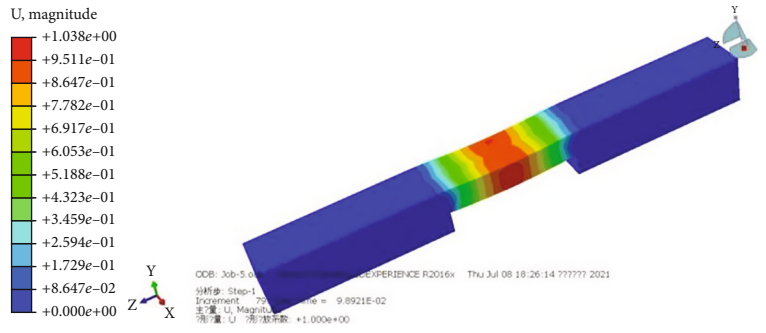

(c) The soil cover layer thickness is 8 m

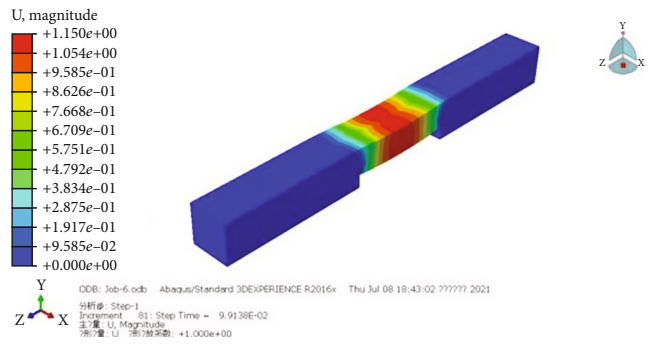

(d) The soil cover layer thickness is 10 m

Figure 9: The soil displacement under different cover layer thicknesses.

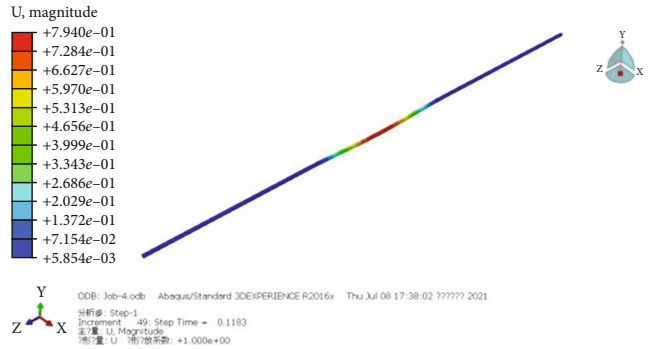

(a) The soil cover layer thickness is 4 m

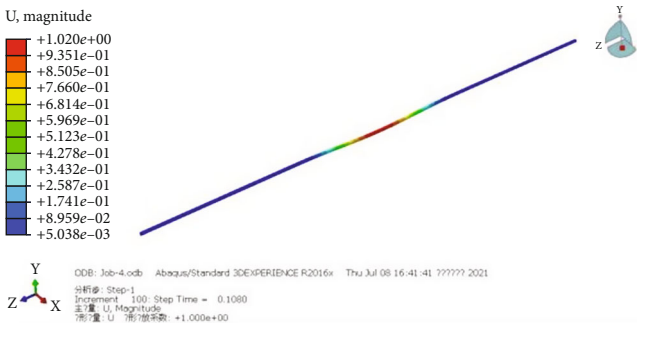

(b) The soil cover layer thickness is 6 m

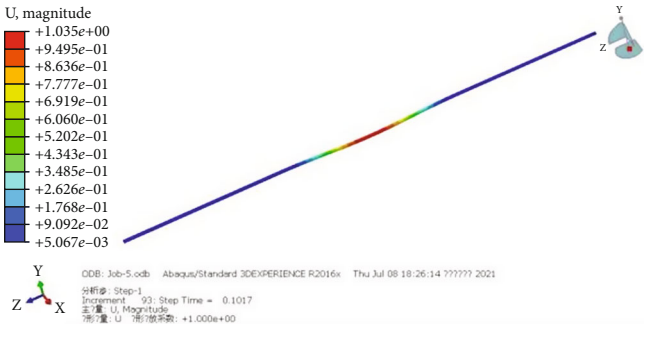

(c) The soil cover layer thickness is 8 m

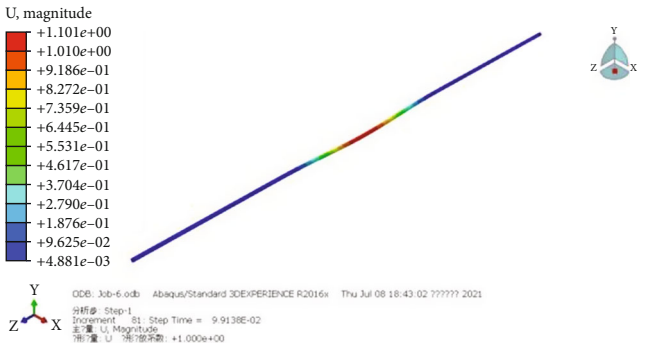

(d) The soil cover layer thickness is 10 m

Figure 10: The pipeline ultimate deformation under different cover layer thicknesses.

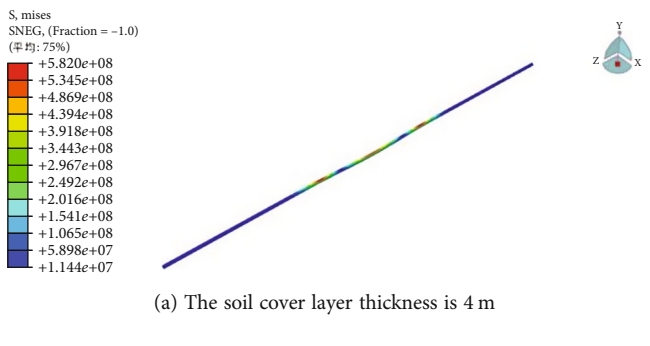

(a) The soil cover layer thickness is 4 m

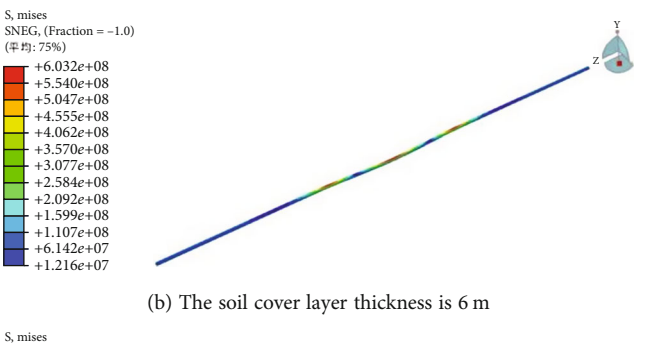

(b) The soil cover layer thickness is 6 m

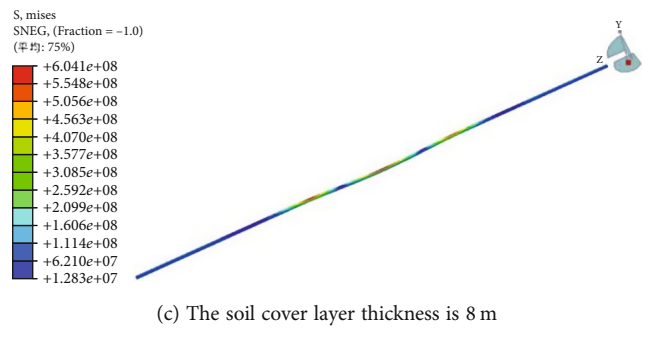

(c) The soil cover layer thickness is 8 m

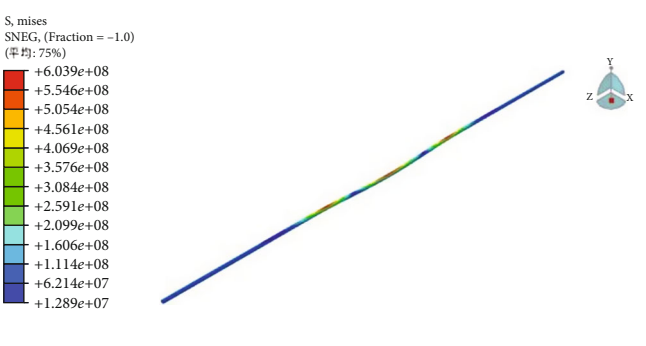

(d) The soil cover layer thickness is 10 m

Figure 11: The pipeline stress under different cover layer thicknesses.

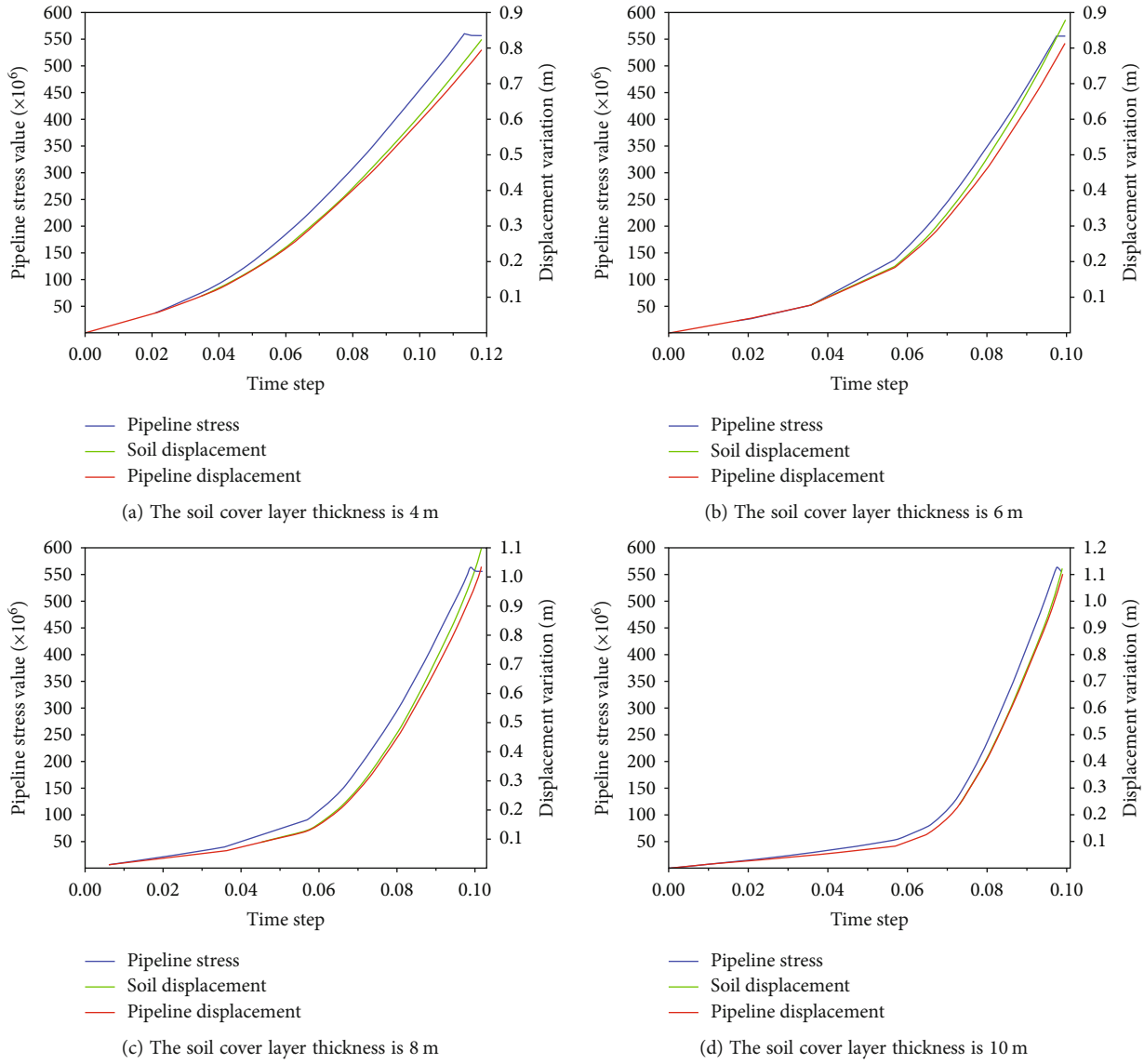

Figure 12: The diagrams of pipeline stress, displacement, and soil displacement under different cover layer thicknesses.

displacement nephograms is basically large in the middle and small in both ends, which is consistent with the maximum displacement variation of soil. When the pipeline reaches the yield strength, the maximum displacement of the pipeline is 1.1 m, and the minimum displacement is 0.79 m, which is smaller than the change of soil displacement.

3.2.3. Analysis of Pipeline Stress under Different Cover Layer Thicknesses. Figure 11 is the stress nephogram of the pipeline under four different cover layer thicknesses. With the increase of cover layer thickness, the maximum equivalent stress distribution of the pipeline is similar, and both the middle and the edge of the collapse area have the largest stress, indicating that there is a certain shear effect. Moreover, in the boundary area of the collapse zone, the displacement is not very large.

After sorting and statistics, the relationship diagrams of pipeline stress, displacement, and soil displacement with calculation time step under different cover layer thicknesses are drawn (Figure 12), and the maximum displacement of the pipeline reaching yield strength under each working condition is extracted (Figure 13).

It can be seen that the stress, displacement, and soil displacement of the pipeline increase slowly first and then increase rapidly, and the maximum stress of the pipeline reaches the yield state, resulting in pipeline failure. With the change of cover layer thickness, the maximum displacement of the pipeline and soil changed little but still increased. Formula ((3)) is obtained by fitting the relationship between the thickness of the cover layer and the maximum displacement of the pipeline, and the fitting degree is 0.9916. According to the expression, the curve grows slowly and the growth acceleration is small.

$$f(x) = 0.003729x^2 - 0.01393x + 0.7846. \quad (3)$$

3.3. Analysis on the Influence of the Pipeline Wall Thickness. In order to study the influence of the pipeline wall thickness on pipeline stress, displacement, and soil displacement, finite

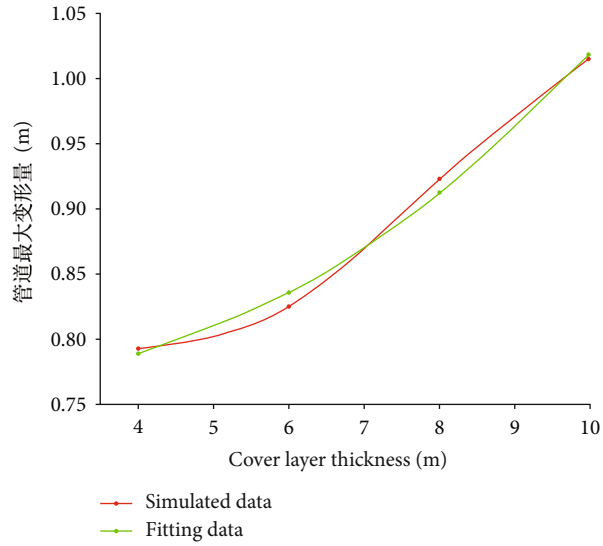

Figure 13: The pipeline maximum displacement under different cover layer thicknesses.

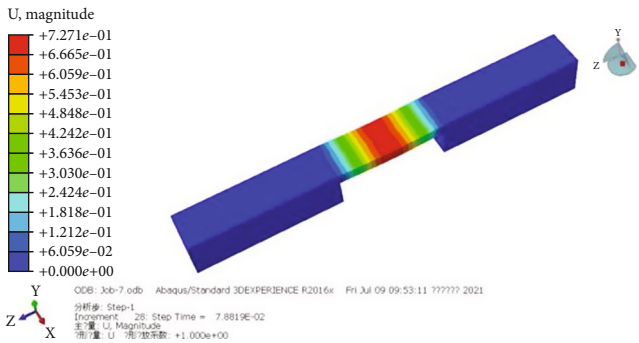

(a) The pipeline wall thickness is 7.9 mm

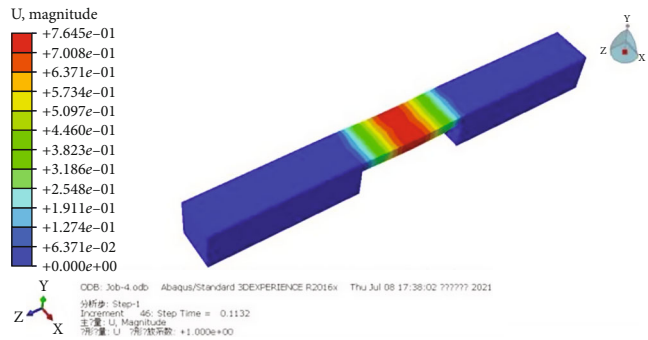

(b) The pipeline wall thickness is 16.2 mm

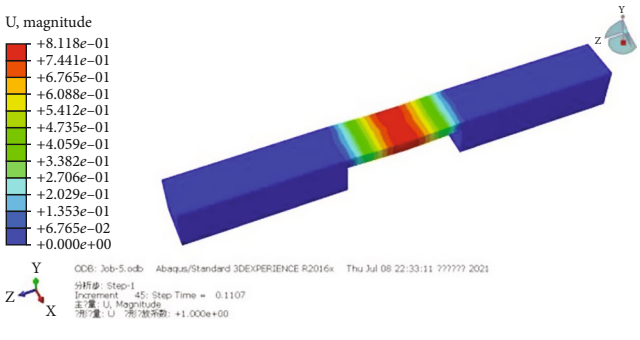

(c) The pipeline wall thickness is18.4 mm

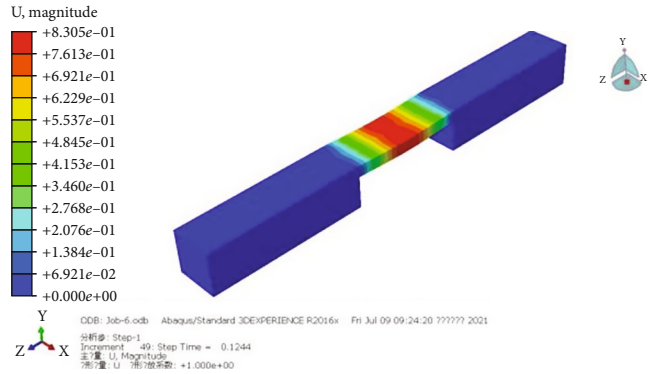

(d) The pipeline wall thickness is 20.6 mm

Figure 14: The soil displacement under different pipeline wall thicknesses.

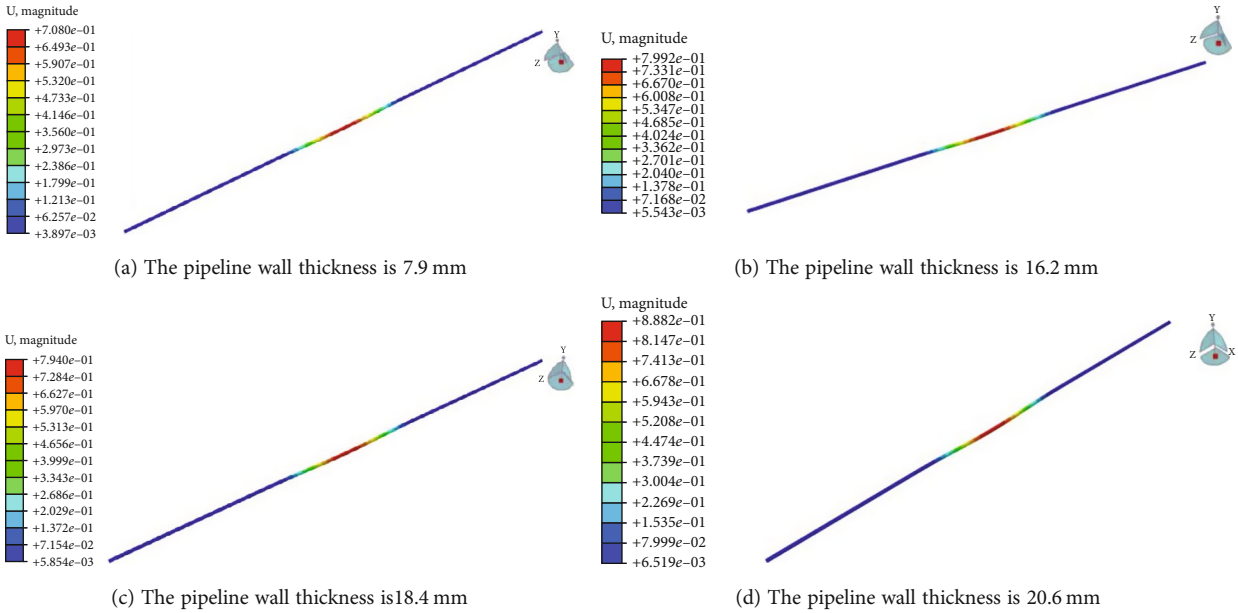

(a) The pipeline wall thickness is 7.9 mm

(b) The pipeline wall thickness is 16.2 mm

(c) The pipeline wall thickness is18.4 mm

(d) The pipeline wall thickness is 20.6 mm

Figure 15: The pipeline ultimate deformation under different pipeline wall thicknesses.

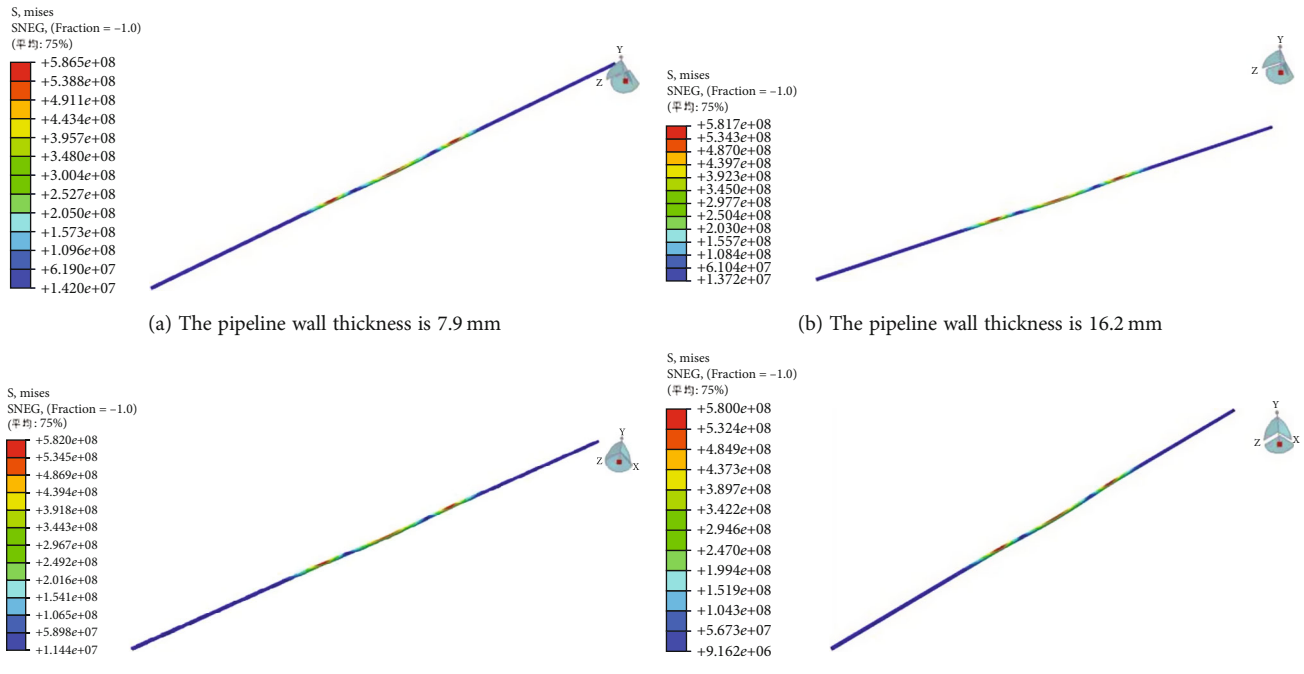

(a) The pipeline wall thickness is 7.9 mm

(b) The pipeline wall thickness is 16.2 mm

(c) The pipeline wall thickness is18.4 mm

(d) The pipeline wall thickness is 20.6 mm

Figure 16: The pipeline stress under different pipeline wall thicknesses.

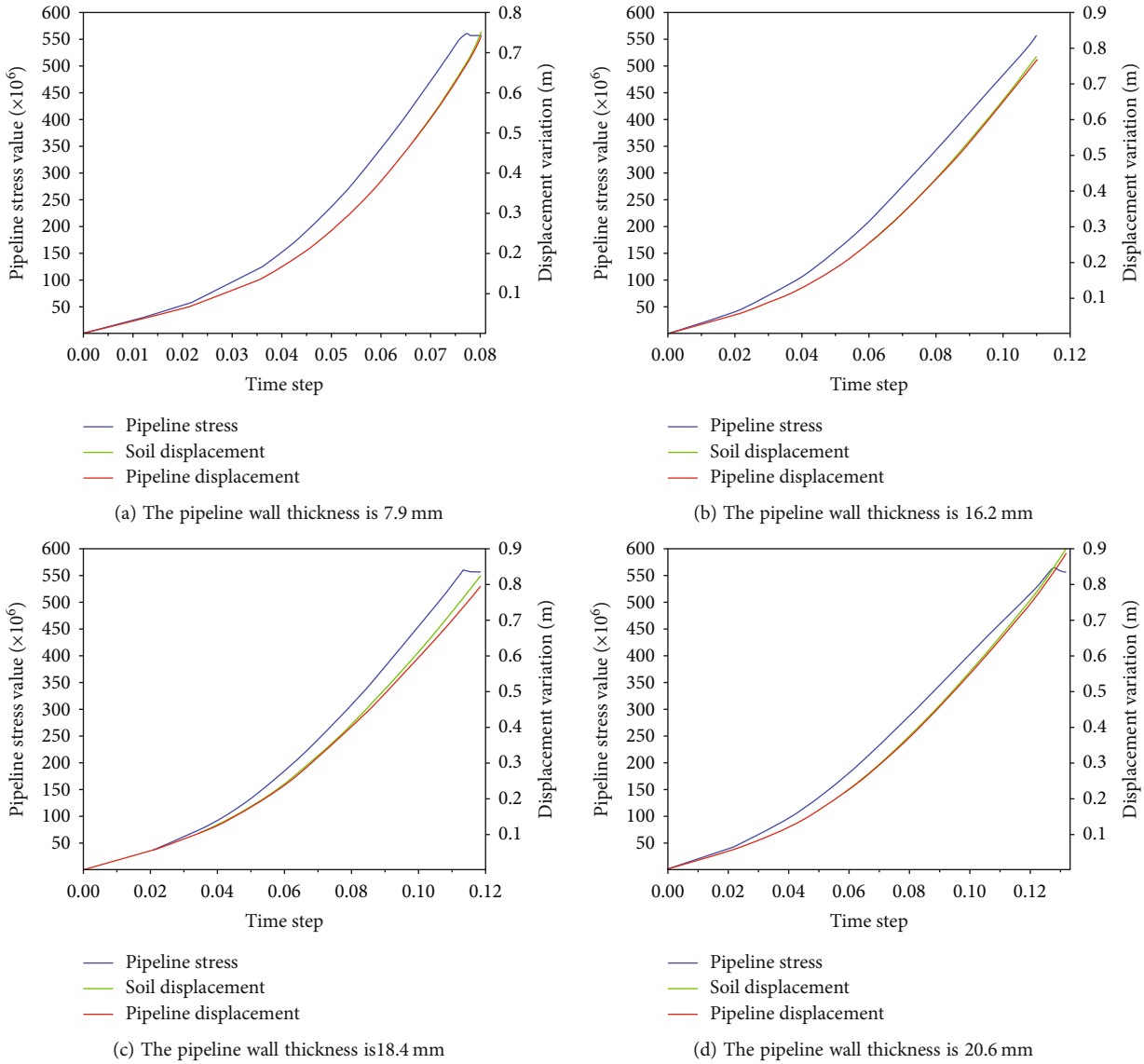

(a) The pipeline wall thickness is 7.9 mm

(b) The pipeline wall thickness is 16.2 mm

(c) The pipeline wall thickness is18.4 mm

(d) The pipeline wall thickness is 20.6 mm

Figure 17: The diagrams of pipeline stress, displacement, and soil displacement under different pipeline wall thicknesses.

element models with pipeline wall thicknesses of 7.9 mm, 16.2 mm, 18.4 mm, and 20.6 mm were established for analysis.

3.3.1. Analysis of Soil Displacement under Different Pipeline Wall Thicknesses. Figure 14 shows the soil displacement nephograms under four different pipe wall thicknesses. It can be seen that different wall thicknesses have little effect on the displacement of soil caused by ground collapse. The maximum displacement of soil under four working conditions is 0.83 m, and the displacement nephograms are basically the same, which is diffused from the center to both sides. When the pipeline wall thickness is 7.9 mm, the soil displacement at the central pipeline position in the collapse area is not the largest, and the displacement on both sides is significantly larger than the central displacement. Moreover, when the outer diameter of the pipeline is constant, the variation of soil displacement slowly increases with the increase of the pipeline wall thickness.

3.3.2. Analysis of Pipeline Ultimate Deformation under Different Pipeline Wall Thicknesses. The maximum displacement of the pipeline under different wall thicknesses is compared in Figure 15. The maximum displacement of the pipeline under yield increases with the increase of wall thickness. As the outer diameter of the pipeline is the same, the increase of wall thickness causes the increase of pipeline gravity and stronger bearing capacity. Under the same conditions, when the pipeline reaches yield, the maximum displacement of the pipeline will also increase. Under different working conditions, the distribution area of displacement variation is similar, which is a large distribution in the middle and small at the two ends.

3.3.3. Analysis of Pipeline Stress under Different Pipeline Wall Thicknesses. Figure 16 shows von Mises stress nephograms of pipelines under four wall thicknesses. It can be seen that the pipeline can reach the yield state under four working conditions, and the distribution law is similar to that of

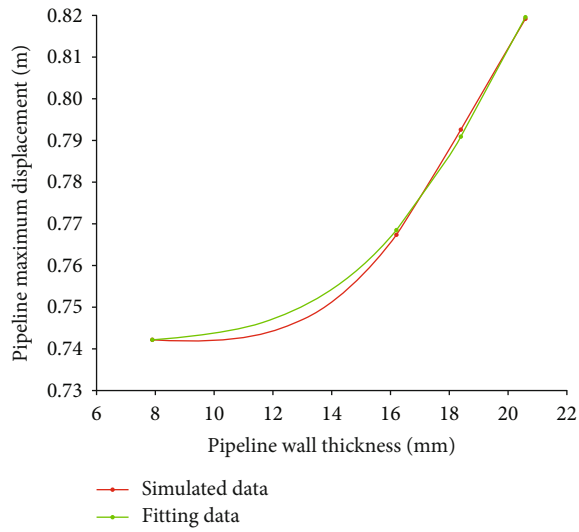

Figure 18: The pipeline maximum displacement under different pipeline wall thicknesses.

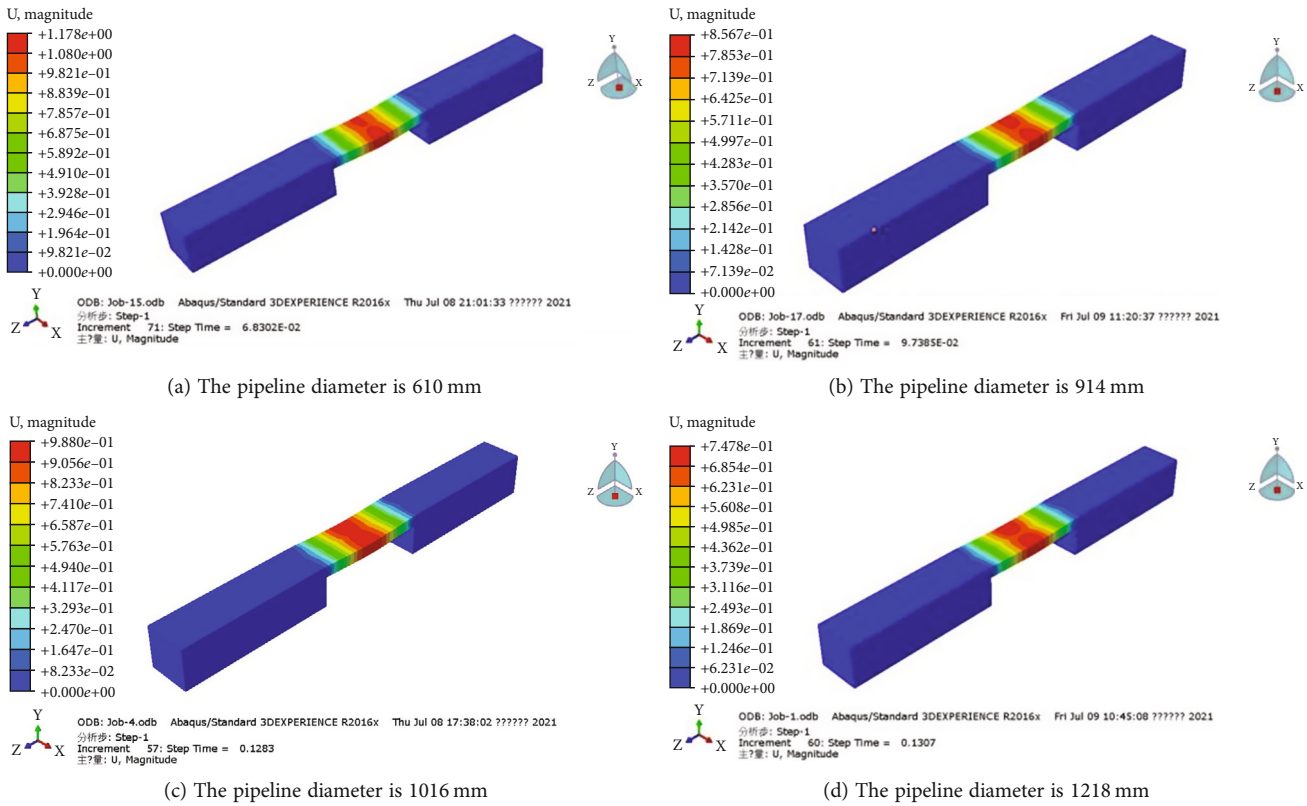

(a) The pipeline diameter is 610 mm

(b) The pipeline diameter is 914 mm

(c) The pipeline diameter is 1016 mm

(d) The pipeline diameter is 1218 mm

Figure 19: The soil displacement under different pipeline diameters.

other working conditions. The stress on the middle and collapse boundary reaches yield first.

The displacement, stress of the pipeline, and displacement of soil with the change of time step are plotted as shown in Figure 17. The maximum displacement of the pipeline is plotted as a curve when the pipeline reaches the yield strength under each wall thickness condition, and the results are shown in Figure 18.

According to the displacement curve, it can be seen that the displacement and stress of pipe-soil change with time step are nonlinear. When the pipeline reaches the yield, there is little difference about the displacement between the pipeline and the soil under different working conditions. The maximum displacement of the pipeline is about 0.84 m, and the minimum is 0.75 m. The pipeline wall thickness changes about 15 mm, and the maximum displacement is only about 0.9 m

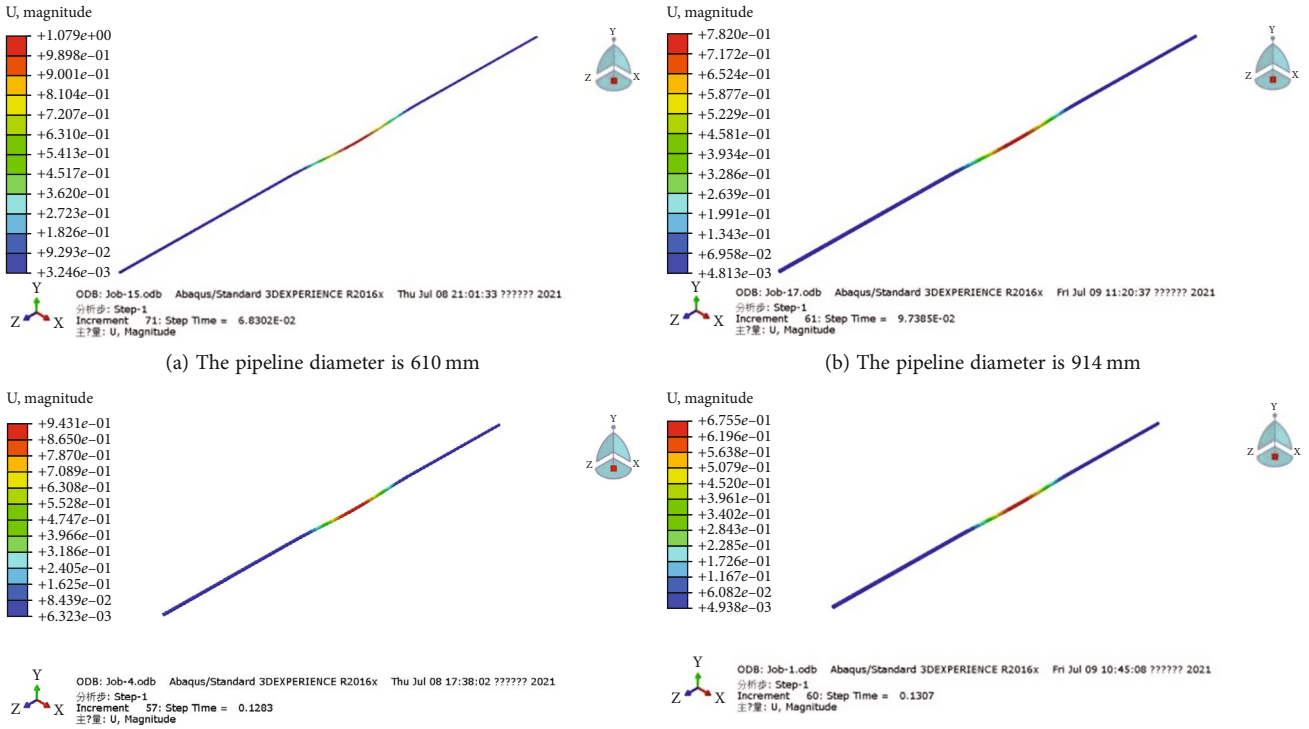

(a) The pipeline diameter is 610 mm

(b) The pipeline diameter is 914 mm

(c) The pipeline diameter is 1016 mm

(d) The pipeline diameter is 1218 mm

Figure 20: The pipeline ultimate deformation under different pipeline diameters.

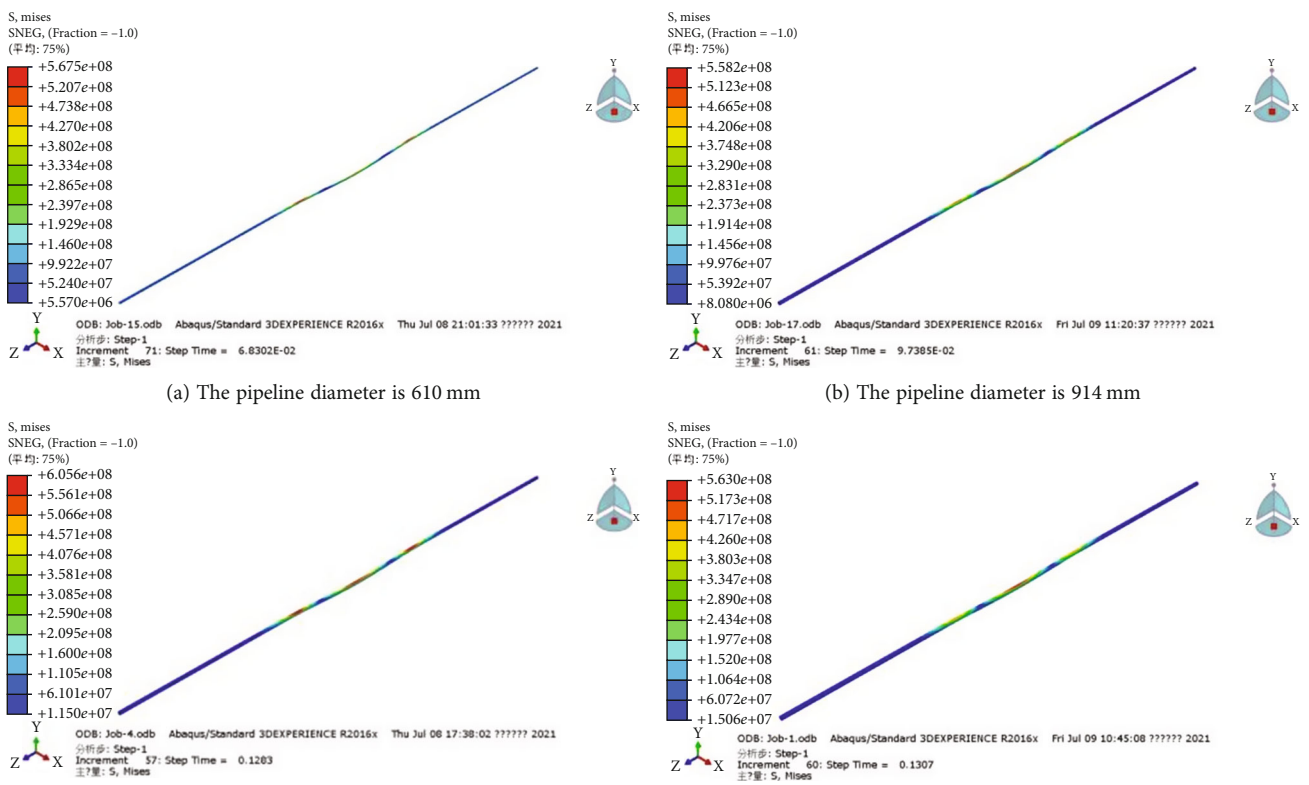

(a) The pipeline diameter is 610 mm

(b) The pipeline diameter is 914 mm

(c) The pipeline diameter is 1016 mm

(d) The pipeline diameter is 1218 mm

Figure 21: The pipeline stress under different pipeline diameters.

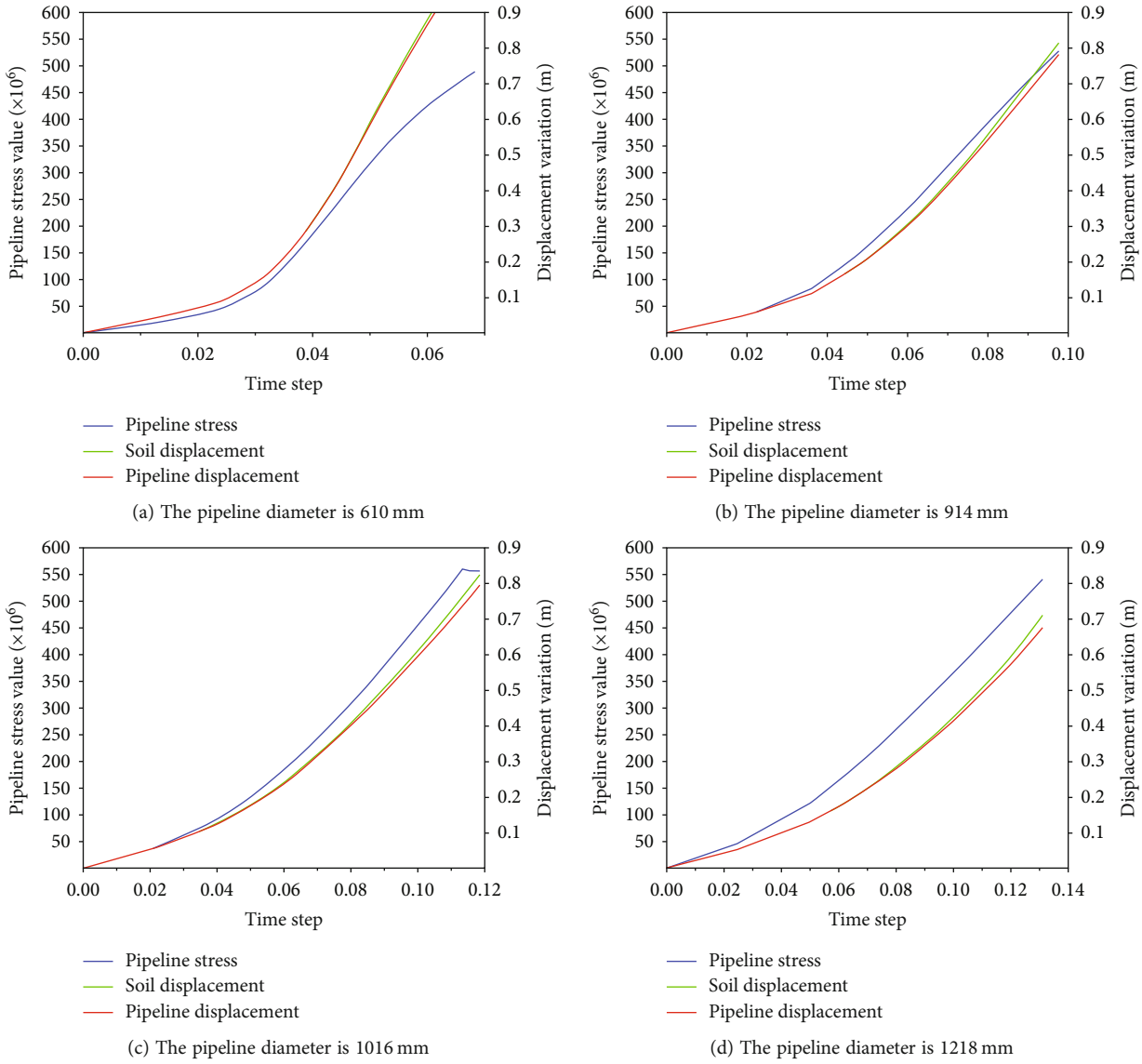

Figure 22: The diagrams of pipeline stress, displacement, and soil displacement under different pipeline diameters.

under yield. It shows that the wall thickness of the pipeline is not the most critical factor to determine the displacement.

From the changing trend of the curve in Figure 18, it can be concluded that if the wall thickness of the pipe is larger, then it is safer, and similarly, the required displacement to reach the yield condition is larger. Therefore, in practical engineering, the mechanical properties and transportation volume of pipelines should be considered comprehensively. In areas with frequent collapses, in addition to considering transport capacity, pipeline strength, economy, etc., the reasonable selection of pipelines with larger wall thickness is conducive to improving the ability of pipelines to resist disasters. Formula ((4)) is obtained by data fitting, and its curve fitting degree is 0.996.

$$f(x) = 0.0006703x^2 - 0.01298x + 0.8028. \quad (4)$$

3.4. Analysis on the Influence of the Pipeline Diameter. In order to study the influence of the pipeline diameter on pipeline stress, displacement, and soil displacement, the finite element models with pipeline diameters of 610 mm, 914 mm, 1016 mm, and 1218 mm were established for analysis.

3.4.1. Analysis of Soil Displacement under Different Pipeline Diameters. Figure 19 shows the soil displacement nephograms under four different pipeline diameters. It can be seen from the figure that when the pipeline diameter is 610 mm, the soil displacement in the middle of the subsidence area is large, and the soil displacement on both sides is small, indicating that the smaller the pipeline diameter, the smaller the upward supporting force on the soil. When the pipeline diameter is 610 mm, the maximum displacement of soil is 1.17 m. When the pipeline diameter is 1218 mm, the maximum displacement of the soil is 0.74 m, indicating that the

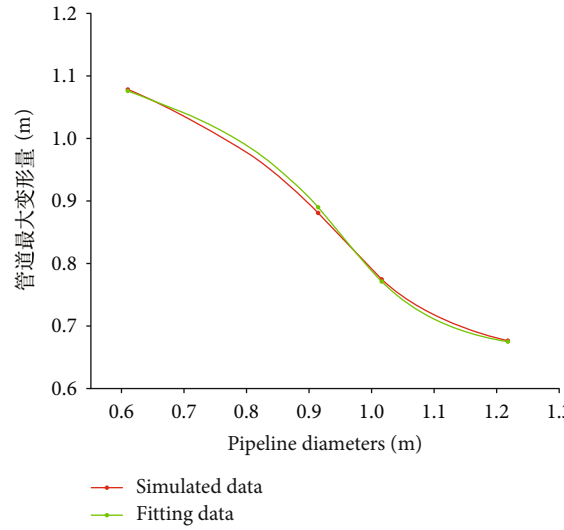

Figure 23: The pipeline maximum displacement under different pipeline diameters.

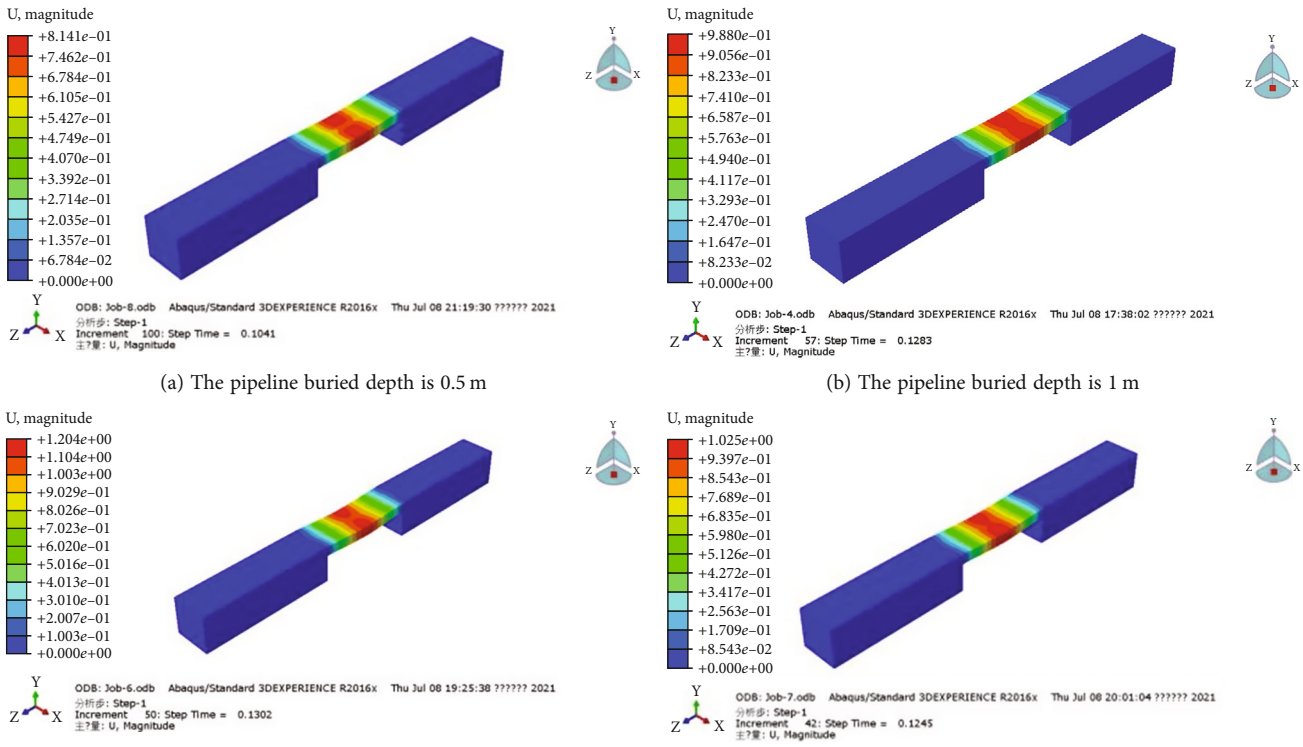

(a) The pipeline buried depth is 0.5 m

(b) The pipeline buried depth is 1 m

(c) The pipeline buried depth is 1.5 m

(d) The pipeline buried depth is 2 m

Figure 24: The soil displacement under different pipeline buried depths.

pipeline diameter has a great influence on the soil deformation. Therefore, in the actual pipeline engineering operation, the pipeline diameter should be reasonably considered.

3.4.2. Analysis of Pipeline Ultimate Deformation under Different Pipeline Diameters. Figure 20 shows the displacement nephograms of pipelines with four different diameters under ground collapse. The displacement nephograms of pipelines show that the two ends are large and the middle is small. If the diameter of the pipe is smaller, the deformation of the pipe will be larger, and the deformation will expand from the center of the pipe to both sides.

3.4.3. Analysis of Pipeline Stress under Different Pipeline Diameters. Figure 21 shows the stress nephogram of pipelines with four different diameters under ground collapse. The

(a) The pipeline buried depth is 0.5 m

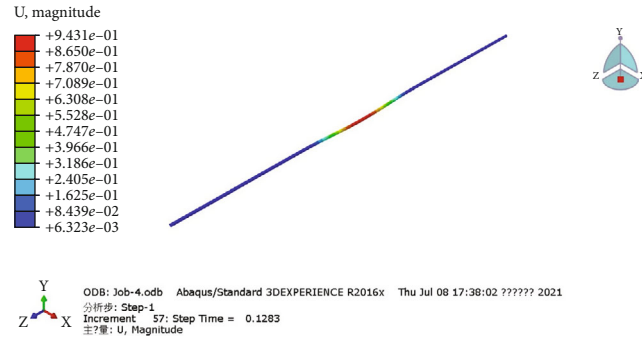

(b) The pipeline buried depth is 1 m

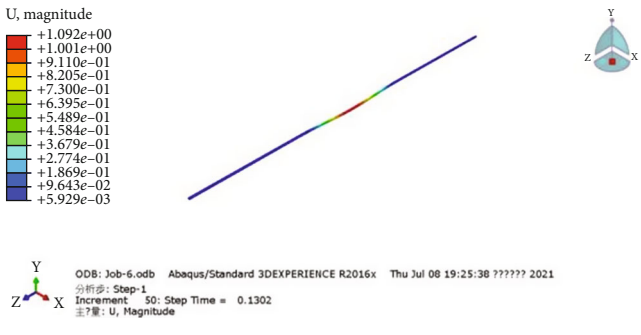

(c) The pipeline buried depth is 1.5 m

(d) The pipeline buried depth is 2 m

Figure 25: The pipeline ultimate deformation under different pipeline buried depths.

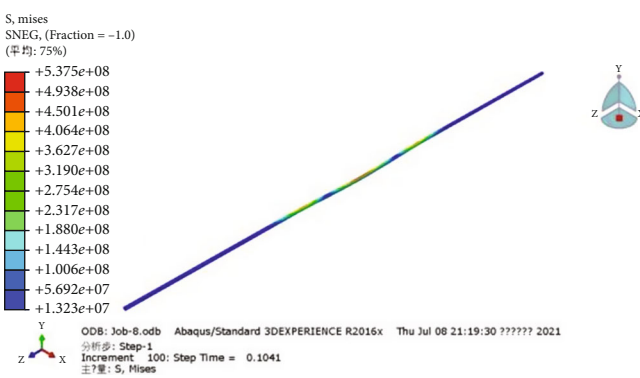

(a) The pipeline buried depth is 0.5 m

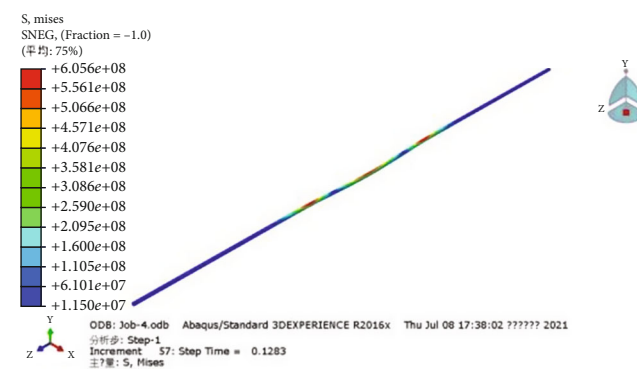

(b) The pipeline buried depth is 1 m

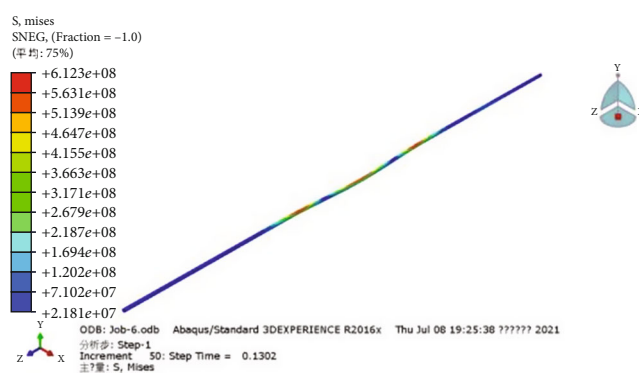

(c) The pipeline buried depth is 1.5 m

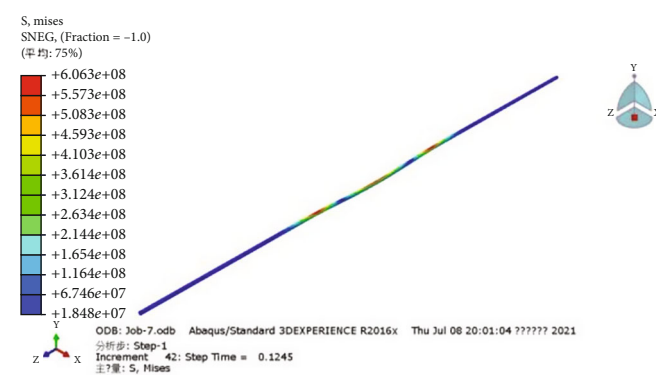

(d) The pipeline buried depth is 2 m

Figure 26: The pipeline stress under different pipeline buried depths.

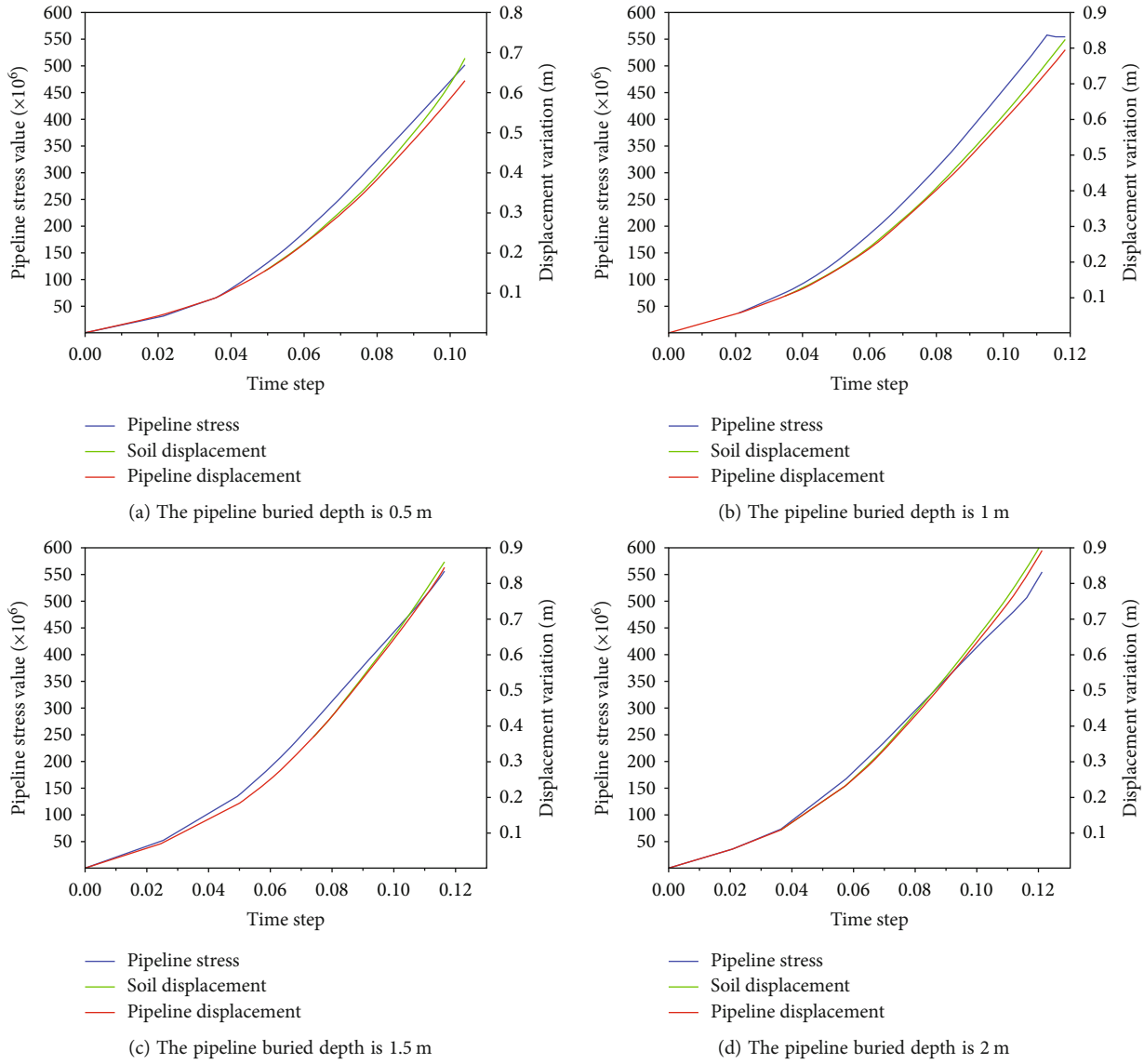

Figure 27: The diagrams of pipeline stress, displacement, and soil displacement under different pipeline buried depths.

calculation is set to reach the yield strength before the calculation is stopped. All pipelines can reach the yield strength. The maximum stress of the pipeline is concentrated in the middle of the pipeline, followed by the edge of the collapse area, and gradually spreads to both sides.

Through data extraction, the variation relationship of pipeline stress, displacement, and soil displacement with time step under different diameters is plotted as shown in Figure 22, and the maximum displacement of the pipeline corresponding to different diameters is made as shown in Figure 23. It can be seen that different pipeline diameters have different times to reach yield strength. If the pipe diameter is smaller, the time for the pipe to reach yield strength is smaller. This is because the smaller the pipeline diameter, the smaller the bending resistance ability of the pipeline and the easier the deformation.

According to the relationship curve of the pipeline maximum displacement under different diameters, the fitting formula (5) is obtained, and the fitting degree is 0.9908. It can be seen that both of them have a linear decreasing relationship. With the increase of the pipeline diameter, the pipeline maximum displacement gradually decreases, and the decreasing speed finally tends to be stable, with a certain linear relationship.

$$f(x) = 1.145x^2 \times 10^{-9} - 0.0009345x + 1.599. \quad (5)$$

3.5. Analysis on the Influence of the Pipeline Buried Depth. In order to study the influence of different buried depths on pipeline stress, displacement, and soil displacement under the action of collapse, the finite element models under four working conditions of 0.5 m, 1 m, 1.5 m, and 2 m buried depth of pipeline are established for analysis.

3.5.1. Analysis of Soil Displacement under Different Pipeline Buried Depths. Figure 24 shows the soil displacement nephograms of four different buried depths of pipelines. It can be seen that with the increase of buried depth, the soil

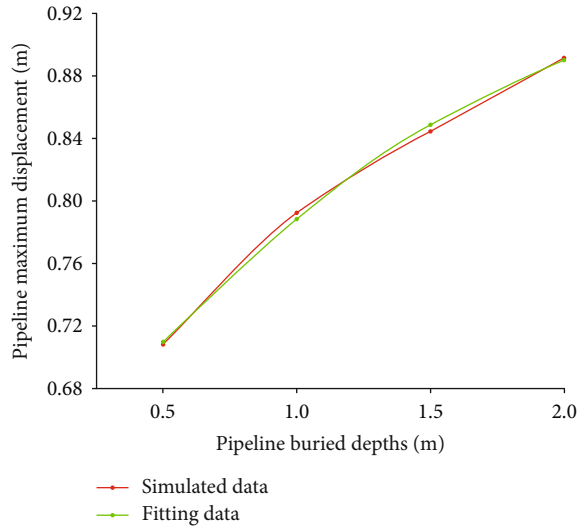

Figure 28: The pipeline maximum displacement under different pipeline buried depths.

displacement gradually increases. Under the action of overburden gravity, if the buried depth of the pipeline is larger, the downward deformation of the pipeline will be larger, and at the same time, the supporting force of the pipeline to the overburden soil will be smaller. The soil displacement decreases gradually from the middle of the subsidence area to both sides.

3.5.2. Analysis of Pipeline Ultimate Deformation under Different Pipeline Buried Depths. Since the simulation is a dynamic process of ground collapse, the intercepted nephograms represent the displacement or equivalent strain of the pipeline in this state. Figure 25 shows the pipeline displacement nephograms with different buried depths under ground collapse. If the buried depth of the pipeline is larger, the weight stress of the overburden soil is larger, and the deformation of the pipeline is larger. The pipeline displacement gradually decreases from the middle to both sides of the collapse area.

3.5.3. Analysis of Pipeline Stress under Different Pipeline Buried Depths. Figure 26 shows the pipeline stress nephogram under ground collapse at different buried depths. Since the calculation is set to stop if the yield strength is reached, all working conditions can reach the yield strength except at a depth of 0.5 m. The distribution law is similar to that of other working conditions, and both the middle and boundary of the collapse zone reach yield first.

Under the condition of ground collapse, the pipeline models of different buried depths can be calculated. The relationship between the pipeline stress, displacement, and soil displacement with the calculation time step can be drawn (Figure 27), and the pipeline's maximum displacement changes under different buried depths can be also drawn (Figure 28).

As shown in Figure 26, if the pipeline buried depth is 0.5 m, the strain and displacement have been increasing, and the strain curve is close to vertical. The calculation time step has far exceeded the time required for other working conditions, resulting in the automatic termination of the calculation by the software, indicating that the pipeline cannot reach the yield strength and will not be destroyed when the pipeline buried depth is 0.5 m. If the buried depth of the pipeline is larger, the displacement difference between the pipeline and soil is smaller. It can be concluded that when the pipeline buried depth is shallow, the pipeline deforms under the action of the overlying soil and has a certain rebound, but its overall deformation shows an upward trend over time. When the pipeline buried depth is large, it is difficult for the pipeline to produce rebound under the action of the overlying soil and to deform together with the upper soil.

According to the relationship curve of the pipeline maximum displacement under different buried depths (Figure 28), the data are fitted to obtain the fitting formula (6), and the fitting degree is 0.9982. It can be seen that both have a linearly increasing relationship. With the increase of buried depth, the maximum displacement of the pipeline increases gradually, which has a certain linear relationship.

$$f(x) = -0.03707x^2 + 0.2141x + 0.6122. \quad (6)$$

4. Analysis of Pipeline Stress Law

4.1. Analysis on Influence Law of Pipeline Deformation. Ground collapse can cause pipeline hanging, even pipeline damage. In the collapse area, the stress state of the pipeline is similar to that of the simply supported beam. The gravity of the pipeline is similar to that of the simply supported beam under uniform load. The effect of the soil at both ends of the collapse area on the pipeline is similar to that of the two ends of the simply supported beam. The lower side of the pipeline is tensile failure, and the boundary stress point of the collapse area is shear failure. The model calculation results under the condition of span length of 40 m are analyzed. In order to better observe the deformation law, the pipeline deformation is amplified by 10 times, and the displacement nephograms are plotted in time step, as shown in Figure 29.

4.2. Analysis of Pipeline Stress Variation. The surrounding soil has certain constraints on the buried pipeline. For many

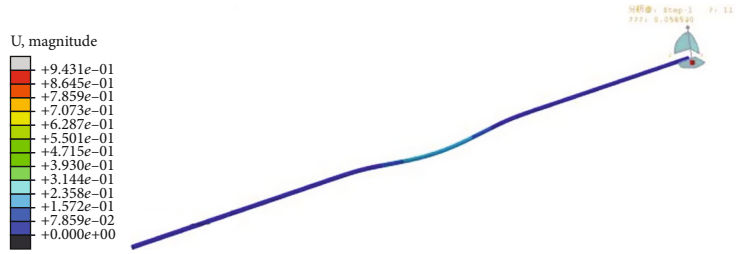

(a) The time step is 0.585

(b) The time step is 0.837

(c) The time step is 0.111

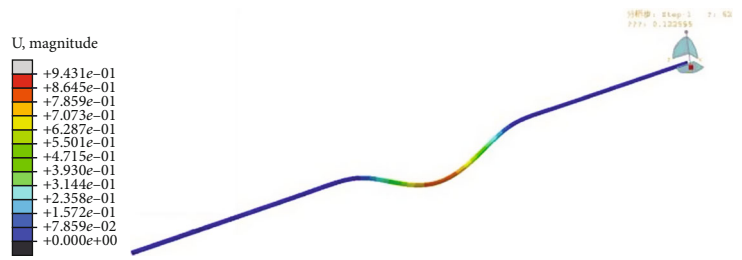

(d) The time step is 0.123

Figure 29: The pipeline deformation at different time steps.

buried pipelines, the collapsed area only occupies a part of the pipeline buried area, and the other part is the noncollapse area. In the analysis of the impact of collapse on buried pipelines, when the foundation subsidence occurs in the area where the pipeline is buried, the resistance of the soil buried under the pipeline to the pipeline is weakened. According to the numerical simulation, the model calculation results under the condition of the 40 m pipeline span are selected. The pipeline stress distribution is amplified by 10 times, and the stress nephograms are truncated according to the time step, as shown in Figure 30.

It can be seen from Figure 30 that the first stress area of the pipeline is located in the center of the pipeline and on both sides of the collapse area, while the stress in the center of the pipeline belongs to tensile stress, and the stress on both sides belongs to shear stress. As the time step progresses, the pipeline stress spreads to both sides.

Different spans have different effects on the stress distribution of pipelines. The longer the span is, the larger the stress variation area is. Under the 120 m span, the entire pipeline appears to show stress increment. With different pipeline wall thicknesses, pipeline diameters, and buried depths, the pipeline maximum stress distribution areas are similar, and they are distributed in the middle and on both sides of the pipeline. According to the stress-time diagram, the pipeline stress is positively correlated and nonlinearly increased with the calculation time step. For the working condition with small span, such as the case of the 20 m span, the stress of the pipeline cannot reach the yield strength, and the soil displacement is much larger than the pipeline deformation, so the pipeline will not be damaged. It indicates that under the influence of different spans, the maximum stress change of the pipeline first tends to be stable and then continues to rise with the increase of the span until the yield strength is reached, and the pipeline is damaged.

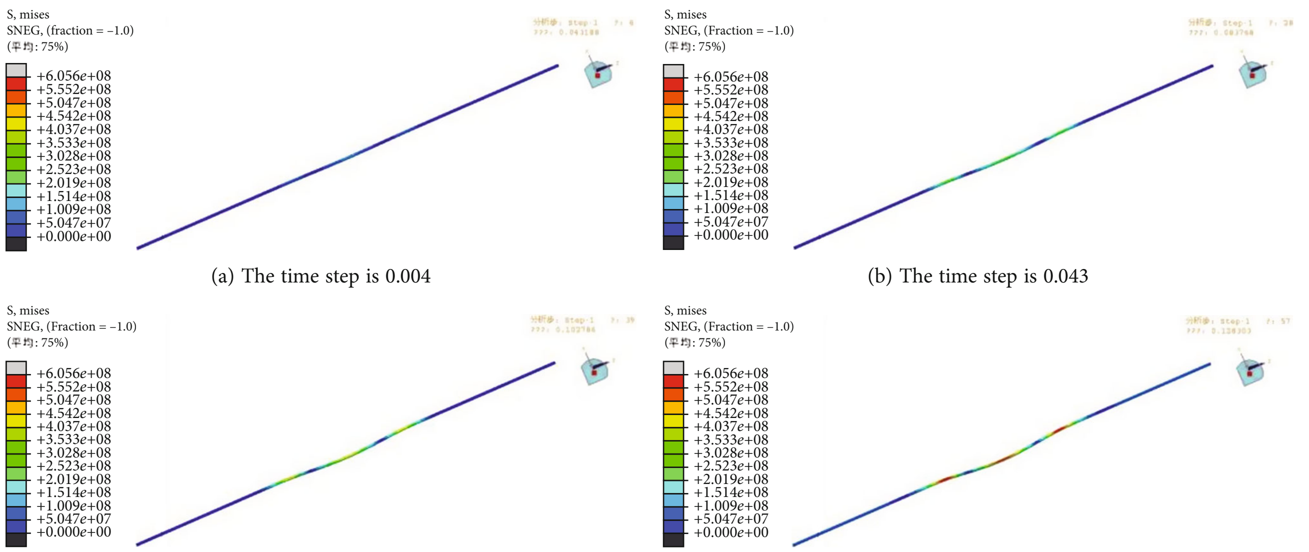

(a) The time step is 0.004

(b) The time step is 0.043

(c) The time step is 0.103

(d) The time step is 0.126

Figure 30: The pipeline stress at different time steps.

5. Conclusions

(1) Under the condition of ground subsidence, ABAQUS is used to simulate the stress-strain situation of pipelines under different pipeline diameters, buried depths, cover thicknesses, spans, and wall thicknesses. The simulation results can reveal the variation law of pipeline stress and strain and have good guiding significance for pipeline safety management and disaster prevention

(2) When the entire collapse area is deformed, the displacement in the middle of the pipeline begins to increase and then expands to both sides, and the center of the pipeline first reaches the yield strength and is destroyed. The deformation area of the pipeline is related to the length, and the deformation amount is not only affected by the length of the collapse area but also related to the diameter of the pipeline, the parameters of the pipeline, and the buried depth. The length of the collapse zone has the greatest influence on the pipe deformation, while the wall thickness and pipe diameter have the least influence

(3) Under the action of ground collapse, the areas where the first stress occurs in the pipeline are located in the center of the pipeline and on both sides of the collapse area. The center of the pipe belongs to tensile stress, and the two sides belong to shear stress. As the pipeline stress spreads to both sides, the pipeline reaches the yield strength and fails, but there is no connection to form a stress change band. Different lengths of the collapse zone have different effects on the overall stress distribution of the pipeline. The longer the length of the collapse zone, the larger the stress change area. With different pipe wall thicknesses, pipe diameters, and buried depths, the maximum stress distribution areas of the pipes are similar, which are distributed in the middle and on both sides, and the pipe stress and time show a positive correlation and nonlinear growth

(4) In this paper, the relationship between the length of the collapse zone, the thickness of the covering layer, the buried depth of the pipeline, the diameter of the pipeline, and the thickness of the pipeline and the maximum deformation of the pipeline are fitted, and the reference value of the maximum displacement of the pipeline under the action of ground collapse is calculated. The work has practical application value for pipeline monitoring, early warning, and disaster management

Data Availability

The data used to support the findings of this study are available from the corresponding author upon request.

Conflicts of Interest

The authors declare that they have no conflicts of interest.

Authors' Contributions

Liu Xiaohui and Sun Zhizhong developed the model; Zhu Jianping and Fang Yingchao collected the data and references; Liu Xiaohui performed data fitting and numerical simulations; and all authors analyzed the results and contributed in writing the manuscript. All authors read and approved the final manuscript.

Acknowledgments

This study was supported by the Applied Research and Development Project of Gansu Academy of Sciences (Grant Nos. 2018JK-14 and 2019JK-05) and Natural Science Foundation of Gansu Province (21JR7RA736).

References

[1] A. Dinar, E. Esteban, E. Calvo et al., "We lose ground: global assessment of land subsidence impact extent," *Science of the Total Environment*, vol. 786, article 147415, 2021.

[2] P. Zhang, G. Qin, and Y. Wang, "Risk assessment system for oil and gas pipelines laid in one ditch based on quantitative risk analysis," *Energies*, vol. 12, no. 6, p. 981, 2019.

[3] Y. Wu, X. You, and S. Zha, "Mechanical behavior analysis of buried polyethylene pipe under land subsidence," *Engineering Failure Analysis*, vol. 108, article 104351, 2020.

[4] S. Oruji, M. Ketabdar, D. Moon, V. Tsao, and M. Ketabdar, "Evaluation of land subsidence hazard on steel natural gas pipelines in California," *Upstream Oil and Gas Technology*, vol. 8, p. 100062, 2022.

[5] D. Liu, J. Yang, X. Wang, J. Zhao, S. Xu, and Y. Zhao, "Experimental study on thermal insulation effect of the buried oil-gas pipelines in permafrost regions," *Geofluids*, vol. 2022, Article ID 4226077, 19 pages, 2022.

[6] Z.-F. Chen, W. P. Chu, H. J. Wang et al., "Structural integrity assessment of hydrogen-mixed natural gas pipelines based on a new multi-parameter failure criterion," *Ocean Engineering*, vol. 247, article 110731, 2022.

[7] D. Wang, P. Zhang, and L. Chen, "Fuzzy fault tree analysis for fire and explosion of crude oil tanks," *Journal of Loss Prevention in the Process Industries*, vol. 26, no. 6, pp. 1390–1398, 2013.

[8] X. Luo, S. Lu, J. Shi, X. Li, and J. Zheng, "Numerical simulation of strength failure of buried polyethylene pipe under foundation settlement," *Engineering Failure Analysis*, vol. 48, pp. 144–152, 2015.

[9] H. Lu, X. Wu, H. Ni, M. Azimi, X. Yan, and Y. Niu, "Stress analysis of urban gas pipeline repaired by inserted hose lining method," *Composites Part B: Engineering*, vol. 183, p. 107657, 2020.

[10] C. Gong and W. Zhou, "First-order reliability method-based system reliability analyses of corroding pipelines considering multiple defects and failure modes," *Structure and Infrastructure Engineering*, vol. 13, no. 11, pp. 1451–1461, 2017.

[11] P. Castellazzi, J. Garfias, and R. Martel, "Assessing the efficiency of mitigation measures to reduce groundwater depletion and related land subsidence in Queretaro (Central Mexico) from decadal InSAR observations," *International Journal of Applied Earth Observation and Geoinformation*, vol. 105, p. 102632, 2021.

[12] J. Wang, Y. Shuai, C. Feng et al., "Multi-dimensional mechanical response of multiple longitudinally aligned dents on pipelines and its effect on pipe integrity," *Thin-Walled Structures*, vol. 166, p. 108020, 2021.

[13] G. E. Muleski, T. Ariman, and C. P. Aumen, "A shell model of a buried pipe in a seismic environment," *Journal of Pressure Vessel Technology*, vol. 101, no. 1, pp. 44–50, 1979.

[14] H. Yun and S. Kyriakides, "Model for beam-mode buckling of buried pipelines," *Journal of Engineering Mechanics*, vol. 111, no. 2, pp. 235–253, 1985.

[15] I. Shmulevich and N. Galili, "Deflections and bending moments in buried pipes," *Journal of Transportation Engineering*, vol. 112, no. 4, pp. 345–357, 1986.

[16] A. Klar, T. E. B. Vorster, K. Soga, and R. J. Mair, "Soil-pipe interaction due to tunnelling: comparison between Winkler and elastic continuum solutions," *Geotechnique*, vol. 55, no. 6, pp. 461–466, 2005.

[17] S. M. Adeeb and D. J. Horsley, "A numerical procedure to establish a safe working pressure during excavation of a pipeline in a rock ditch," *International Journal of Pressure Vessels and Piping*, vol. 83, no. 7, pp. 488–497, 2006.

[18] O. Kinash and M. Najafi, "Large-diameter pipe subjected to landslide loads," *Journal of Pipeline Systems Engineering and Practice*, vol. 3, no. 1, pp. 1–7, 2012.

[19] M. Saiyar, P. Ni, W. A. Take, and I. D. Moore, "Response of pipelines of differing flexural stiffness to normal faulting," *Geotechnique*, vol. 66, no. 4, pp. 275–286, 2016.

[20] M. V. Shruthi, "Seismic response of buried pipe lines and preparation of seismic resistant joint," *International Journal of Civil Engineering and Technology*, vol. 8, pp. 1563–1575, 2017.

[21] C. Varianou Mikellidou, L. M. Shakou, G. Boustras, and C. Dimopoulos, "Energy critical infrastructures at risk from climate change: a state of the art review," *Safety Science*, vol. 110, pp. 110–120, 2018.

[22] Y. Wu, X. You, and S. Zha, "Investigation of mechanical behavior of buried DN110 polyethylene pipe with a scratch defect under land subsidence," *Engineering Failure Analysis*, vol. 125, article 105371, 2021.

[23] Y. Wang, P. Zhang, and G. Qin, "Non-probabilistic time-dependent reliability analysis for suspended pipeline with corrosion defects based on interval model," *Process Safety and Environmental Protection*, vol. 124, pp. 290–298, 2019.

[24] C. Wong, R. G. Wan, and R. C. K. Wong, "Performance of buried pipes in moving slopes under axial loading - evaluation tools," *Journal of Pipeline Science and Engineering*, vol. 1, no. 2, pp. 167–175, 2021.

[25] Y. Wang, P. Zhang, X. Q. Hou, and G. Qin, "Failure probability assessment and prediction of corroded pipeline under earthquake by introducing in-line inspection data," *Engineering Failure Analysis*, vol. 115, p. 104607, 2020.

[26] H. Wang, J. Xu, X. Liu, and L. Sheng, "Preparation of straw activated carbon and its application in wastewater treatment: a review," *Journal of Cleaner Production*, vol. 283, p. 124671, 2021.

[27] M. Sahlabadi and N. Soltani, "Experimental and numerical investigations of mixed-mode ductile fracture in high-density polyethylene," *Archive of Applied Mechanics*, vol. 88, no. 6, pp. 933–942, 2018.

[28] C. Gong and W. Zhou, "Importance sampling-based system reliability analysis of corroding pipelines considering multiple failure modes," *Reliability Engineering and System Safety*, vol. 169, pp. 199–208, 2018.

[29] X. Liu, M. Zhang, Z. Sun, H. Zhang, and Y. Zhang, "Comprehensive evaluation of loess collapsibility of oil and gas pipeline based on cloud theory," *Scientific Reports*, vol. 11, no. 1, article 15422, 2021.

[30] D. Pan, *Stress analysis of gas pipeline in a karst collapse area of Guangxi*, Master Dissertation, Southwest Petroleum University, 2018.